


**ANALYZING RAINFALL THRESHOLDS  
FOR SHALLOW LANDSLIDES USING  
SATELLITE REMOTE SENSING AND  
PHYSICALLY-BASED MODELING. A  
CASE STUDY FROM RASUWA DISTRICT,  
NEPAL**

BIN GUO  
March 2017

SUPERVISORS:  
Dr. Cees. van Westen  
Dr. Janneke. Ettema  
Dr. Olga. Mavrouli  
Drs. Nanette. Kingma



# **ANALYZING RAINFALL THRESHOLDS FOR SHALLOW LANDSLIDES USING SATELLITE REMOTE SENSING AND PHYSICALLY-BASED MODELING. A CASE STUDY FROM RASUWA DISTRICT, NEPAL**

**BIN GUO**

**Enschede, The Netherlands, March, 2017**

Thesis submitted to the Faculty of Geo-Information Science and Earth Observation of the University of Twente in partial fulfilment of the requirements for the degree of Master of Science in Geo-information Science and Earth Observation.

Specialization: Applied Earth Sciences – Natural Hazards and Disaster Risk Management (AES-NHSRM)

**SUPERVISORS:**

Dr. Cees. van Westen

Dr. Janneke. Ettema

Dr. Olga. Mavrouli

Drs. Nanette. Kingma

**THESIS ASSESSMENT BOARD:**

Prof. Dr. Freek van der Meer

Dr. Rens van Beek (External Examiner, Utrecht University)

etc

#### DISCLAIMER

This document describes work undertaken as part of a programme of study at the Faculty of Geo-Information Science and Earth Observation of the University of Twente. All views and opinions expressed therein remain the sole responsibility of the author, and do not necessarily represent those of the Faculty.

## ABSTRACT

On 25 April 2015, an M7.8 large earthquake happened in Nepal and 4312 landslides were triggered during or after the earthquake. The 2015 earthquake already past for almost two years, but the risk of rainfall-induced landslides is still high in Nepal. The rainfall-induced shallow landslides threaten both human lives and economy development, especially in Rasuwa area. A regional scale Early Warning System (EWS) can be an effective method to reduce the hazards.

The general objective of this thesis is the development of rainfall thresholds as a component of a regional Landslide Early Warning System using satellite-derived rainfall in combination with physically-based landslide initiation modelling for a test area in Nepal.

Multiple rainfall data analysis was carried out mainly based on Pearson correlation coefficient and significance calculation. Global Precipitation Measurement (GPM) data have a better performance in this area, while the calibration work cannot be finished because of the limitation of data. The maximal value of the rainfall station data and GPM data was used as input. The soil depth is stimulated by using the soil depth model. Small modifications were done to add extra depth related to land use and historical landslides. The parameterization with limited information is mainly relaid on literature data as there was no possibility to carry out sufficient field and laboratory testing.

The main methodology of rainfall threshold definition is STARWARS+PROBSTAB physically-based model. Dynamic hydrological model STARWARS provide the soil moisture and groundwater change, and infinite slope stability model PROBSTAB produce the factor of safety. Several modification have been done to adjust the model into study area. 2015 rainfall scenario was set as the rainfall input. The model output could not be validated with historical landslide dates and locations, as these were not available. Therefore the results were checked by analyzing the results from four specific points. The model results of 2015 show the same trend as real conditions based on filed observations.

Two types of rainfall thresholds were defined based on the physically-based modelling, intensity-duration threshold (I-D) and intensity-antecedent rainfall threshold (I-A). Accurate slope failure time and location cannot be simulated by the model, the percentage of the unstable areas were used in threshold definition instead. No validation had been done to test the thresholds. Because no accurate landslides dates that matched with the triggering rainfall were available.

**Keywords:** early warning system, rainfall threshold, shallow landslide, satellite rainfall data, soil depth model, Nepal.

## ACKNOWLEDGEMENTS

First and foremost, I would like to express my gratitude to ITC for giving me the chance to study here and providing the scholarship. Also I would like to thank Prof Runqiu Huang and Prof Xiangjun Pei in Chengdu University of Technology for supporting my MSc study in ITC.

I am deeply grateful for my supervisors, Dr. Cees van Westen, Dr. Janneke Ettema, Dr. Olga Mavrouli, and Drs. Nanette Kingma. I can never finish the thesis without their help. The intelligent guidance, warm encouragement, and powerful support are pushing me to accomplish the research.

I am sincerely thankful for Dr. Jianqiang Zhang and PhD candidate Bastian van de Bout. Thanks for spend so much time on helping me and your advices are really helpful.

I would like to appreciate Dr. Rens van Beek for providing me the STARWARS+PROBSTAB model, appreciate Constanza Maass Morales and Francisco Zambra for giving me the script for rainfall satellite data.

I would also like to appreciate Susmita Dhakal, Radhika Maharjan, Acharya Akash and all the people that give us help in Nepal.

I would like to thank all the members in Nepal group: Sohel Rana, Sansar Meena, Dinorah Pantle Cebada. Our group work is the foundation of the study and I will never forget the days in Nepal.

I would like to thank all my Chinese friend in ITC who give me support and company through the unforgettable 18 months.

I would like to thank all the teachers and classmates in ESA department, all the time we spent together was great.

Finally, I want give many thanks to my dear parents and girlfriend for their unconditional love, patience, and support. I cannot go through everything without you.

## TABLE OF CONTENTS

---

1.	Introduction.....	1
1.1.	Background.....	1
1.2.	Problem statement.....	1
1.3.	Literature review.....	2
1.4.	Objectives.....	3
1.5.	Methodology.....	4
2.	Study area.....	7
2.1.	Location and general description.....	7
2.2.	Climate.....	8
2.3.	Landslide condition.....	9
2.4.	Field work.....	10
3.	Rainfall data analysis.....	13
3.1.	Introduction.....	13
3.2.	Daily rainfall.....	13
3.3.	Satellite based precipitation comparison.....	16
3.4.	Comparing ground stations with satellite products.....	18
3.5.	Conclusion.....	19
4.	Soil data analysis.....	20
4.1.	Introduction.....	20
4.2.	Soil depth model.....	21
4.3.	Soil related parameters.....	25
5.	Rainfall thresholds definition using physically-based modelling.....	28
5.1.	Introduction.....	28
5.2.	Model results.....	29
5.3.	Intensity-duration rainfall threshold definition.....	34
5.4.	Intensity-antecedent rainfall threshold definition.....	36
5.5.	Summary.....	41
6.	Discussion, Conclusion, and suggestion.....	42
6.1.	Discussion.....	42
6.2.	Conclusion.....	43
6.3.	Suggestion.....	44
	List of references.....	45
	Appendix.....	48

## LIST OF FIGURES

Figure 1-1 Flow chart of methodology.....	6
Figure 2-1 Valley-blocking landslides (Pink spot) after 2015 earthquake in Nepal, Rasuwa in red boundary (Collins & Jibson, 2015). .....	7
Figure 2-2 a, b. The houses and cars destroyed by co-seismic landslides.....	8
Figure 2-3 The India Monsoon Onset Map (Burrongs, 1999) red star represent Rasuwa area.....	8
Figure 2-4 Average high and low temperature of Rasuwa (2000-2012) source: world weather online .....	9
Figure 2-5 Average monthly precipitation and raining days (2000-2012) source: world weather online .....	9
Figure 2-6 Landslide susceptibility map of Rasuwa, Nepal (DRRP, 2016).....	9
Figure 2-7 Mosaic base map of study area.....	10
Figure 2-8 Land cover map of study area .....	10
Figure 2-9 Co-seismic landslide mapping based on Google earth and field investigation.....	11
Figure 2-10 Rainfall-induced landslide mapping based on Google earth and field investigation .....	11
Figure 2-11 Soil depth investigation points .....	12
Figure 3-1 Location of rainfall stations near study area (source: Google earth).....	13
Figure 3-2 Correlation between latitude and maximal daily precipitation of 2015.....	15
Figure 3-3 Correlation between latitude and sum precipitation of 2015.....	15
Figure 3-4 Scatter between station 1017 and 1004.....	15
Figure 3-5 Scatter between station 1017 and 1001.....	15
Figure 3-6 Pixel of TRMM data near study area.....	16
Figure 3-7 Pixels of GPM data near study area.....	16
Figure 3-8 The daily precipitation derived from TRMM (2015 monsoon) .....	16
Figure 3-9 The daily precipitation derived from GPM pixel 9 (2015 monsoon).....	16
Figure 3-10 Scatter plot between GPM pixel 8 and TRMM.....	18
Figure 3-11 Scatter plot between GPM pixel 8 and 9.....	18
Figure 3-12 Daily precipitation scatter between station 1001 and GPM pixel 2 .....	19
Figure 3-13 5-day precipitation scatter between station 1001 and GPM pixel 2 .....	19
Figure 3-14 10-day precipitation scatter between station 1001 and GPM pixel 2 .....	19
Figure 3-15 15-day precipitation scatter between station 1001 and GPM pixel 2.....	19
Figure 4-1 DEM map used in the model.....	22
Figure 4-2 Soil depth map of original model.....	22
Figure 4-3 Classified land cover map.....	22
Figure 4-4 Debris slides deposit in Rasuwa.....	23
Figure 4-5 Rock fall deposit in Rasuwa .....	23
Figure 4-6 Flow chart of extra soil depth.....	23
Figure 4-7 Soil depth map of improved model.....	24
Figure 4-8 Scatters of original soil depth model and field data .....	25
Figure 4-9 Scatters if improved soil depth model and field data .....	25
Figure 4-10 Soil water characteristics model.....	25
Figure 4-11 Curve of cohesion and water content .....	26
Figure 5-1 Mechanism of rainfall-induced landslides.....	28
Figure 5-2 Modified 2015 daily rainfall and percentage of FOS<1 .....	30
Figure 5-3 Unstable area under 2015 rainfall condition.....	30
Figure 5-4 Number of unstable days .....	31
Figure 5-5 rainfall-induced landslides and areas that FOS<1.....	31

Figure 5-6 a-d The groundwater level, soil moisture, and factor of safe curve during 2015 monsoon of point 1 in unstable bare land.....	32
Figure 5-7 a-d The groundwater level, soil moisture, and factor of safe curve during 2015 monsoon of point 2 in unstable farmland .....	32
Figure 5-8 a-d The groundwater level, soil moisture, and factor of safe curve during 2015 monsoon of point 3 in stable farmland.....	33
Figure 5-9 a-d The groundwater level, soil moisture, and factor of safe curve during 2015 monsoon of point 3 in stable forest.....	33
Figure 5-10 The result of model. Numbers of unstable pixels (FOS<1) change.....	35
Figure 5-11 The I-D rainfall thresholds.....	35
Figure 5-12 Threshold of Dabal (2008), Mathew (2014), and present study.....	36
Figure 5-13 I-A rainfall threshold defined by Gabet et al (2004).....	37
Figure 5-14 Different antecedent rainfall curves.....	38
Figure 5-15 a, b, c The scatter graph of 5-day, 10-day, 30-days antecedent versus daily rainfall. The points show the percentage of unstable pixels during the year 2015.....	39
Figure 5-16 The landslides triggered by first two weeks of 2016 monsoon .....	40
Figure 5-17 Validation using first two week rainfall data from 2016 monsoon .....	41



## LIST OF TABLES

---

<i>Table 3-1 Rainfall stations information.....</i>	14
<i>Table 3-2 Pearson correlation coefficient and significant of rainfall stations.....</i>	14
<i>Table 3-3 information of satellite rainfall products (NASA website).....</i>	16
<i>Table 3-4 PCC and sig between GPM pixel 1 to 9 and TRMM data.....</i>	17
<i>Table 3-5 Sum rainfall and Max daily rainfall of 2015 monsoon season.....</i>	18
<i>Table 3-6 Correlation between station 1001 and GPM pixel 2.....</i>	18
<i>Table 4-1 Shear strength of different gravel content (Yang, 2013).....</i>	20
<i>Table 4-2 Cohesion under different soil moisture (Yang, 2013).....</i>	20
<i>Table 4-3 Maxima root cohesion of different root condition (Gai, 2013).....</i>	20
<i>Table 4-4 Calibration constants of soil depth model.....</i>	21
<i>Table 4-5 Different extra depth of different LULC.....</i>	23
<i>Table 4-6 Different extra depth of different landslides.....</i>	23
<i>Table 4-7 Field investigation record and model product.....</i>	24
<i>Table 4-8 Correlation analysis of soil depth model.....</i>	24
<i>Table 4-9 Ksat of soil test results and model results.....</i>	26
<i>Table 4-10 Ksat of different land cover classes.....</i>	26
<i>Table 4-11 Other parameter values and their sources.....</i>	27
<i>Table 4-12 Maximal root cohesion of different vegetation condition.....</i>	27
<i>Table 4-13 Input initial conditions.....</i>	27
<i>Table 5-1 Validation points information.....</i>	32

# 1. INTRODUCTION

## 1.1. Background

Nepal is located in south side of Himalaya Mountains, the impact between Tibetan plate and India plate causes frequent and strong tectonic movement in this area. Besides the highest mountain in the world, the tectonic movements also bring Nepal complex geological conditions and active seismic events. The plate collision increase the possibility of earthquake, developed joints and fractures in the rock mass make the slope structure more vulnerable, the summer monsoon brings abundant precipitation. All these factors make contributions to the occurrence of geo-hazards especially landslides.

According to the statistical data from Nepal disaster reports, there were 2942 landslides recorded between 1971 and 2012. Duration these landslides, 4511 people died, 1566 injured and more than 555,000 families are affected. And due to the environment and climate change, 219 people and 241 people died because of floods and landslides. (Dhakal, 2016)(MoHA, DPNet, 2011, 2013, 2015)

On 25 April 2015, an M7.8 large earthquake happened in Nepal and followed by more than 250 aftershocks which  $>M$  3.0. More than 9000 people got killed in this catastrophe. 4312 landslides were triggered during or after the earthquake. 491 glacier lakes were found. Human lives and properties are endangered. (Collins & Jibson, 2015)

This extreme seismic event produced plenty of loose material and cracks all over the mountain area. It will take less precipitation to trigger a landslide. After the extreme precipitation in the ongoing monsoon season, the occurrence of shallow landslides increase dramatically and many of the antecedent landslides are reactivated. This condition also evidenced after other earthquakes, like Chi-Chi and Wenchuan earthquake (Lin et al., 2006; Tang et al., 2009). The rainfall thresholds will change after a major event because the powerful seismic movement destroyed slope structure and left loose material on the slope surface. People and villages are endangered.

## 1.2. Problem statement

The 2015 earthquake already past for almost two years, but the risk of rainfall-induced landslides is still high in Nepal. The rainfall-induced shallow landslides threaten both human lives and economy development, especially in Rasuwa area. Risk reduction measures must be taken in this region. Engineering methods are very common and effective way of landslide risk reduction. Retaining wall and dam can dramatically increase the slope stability and protect the buildings and roads. However, the steep slope and loose soil condition increase the difficulty of engineering methods. Another obstacle is financial problem, reconstruction and relocation after the earthquake already spent a large sum of money. The economic condition cannot afford the construction. The viaduct has been widely used in high way construction in Wenchuan area, China. This kind of highway can avoid the influence of landslides, but the expense is also very high. Ecological methods are more cost-effective in risk reduction, but vegetation needs time to grow and maintenance. A regional scale Early Warning System (EWS) can be an effective method to reduce the hazards. An effective EWS can send the alarm message to local community or government, people will prepare or evacuate from the dangerous area.

Because of the limitation of time and energy, an integrated EWS is overambitious for an MSc thesis. The rainfall threshold will be the main objective of this research.

### 1.3. Literature review

EWSs have been widely used in geo-hazards in many countries. (Liu et al., 2016) developed an EWS in Wenchuan area that also affected by the earthquake. There is also an active EWS in Nepal, which is a community-based flood EWS for Rapti River Basin (Gautam & Phaiju, 2013). Early warning system (EWS) is a combination of hazards analysis, monitoring, threshold definition, alert, and social response (Fallis, 2013). Threshold is the basis of the alert, the alert will be sent to people when the monitoring index exceeding a certain pre-defined threshold (Staehli et al., 2015). The definition of the threshold will be based on hazards analysis. Initially, EWSs were designed to deal with simple rainfall related hazards such as flood and drought, but now experts are applying this technology to more complex hazards like landslides.

Thresholds are used to indicate the stability or probability of occurrence of landslides. There are two general methods of threshold definition statistical analysis and physically-based analysis. Statistical analysis based on historical rainfall data and landslide events. The threshold will be defined by the relationship between landslide occurrence and antecedent rainfall or cumulated rainfall. Intensity-Duration thresholds are the most common rainfall threshold definition. Galanti et al (2016) defined a rainfall threshold for shallow landslides in Italy based on statistical methods. In the review paper done by Guzzetti et al (2008), rainfall thresholds for shallow landslides and debris flow for many parts in the world are discussed. They present rainfall thresholds of different time, different events, and different areas. There are also rainfall thresholds studies for the Himalaya region. Mathew et al (2013) generated rainfall threshold for rainfall-induced landslides in Garhwal Himalaya, India using TRMM data. Dahal & Hasegawa (2008) developed rainfall threshold for the whole Nepal area. 193 landslides and matched rainfall events are used in the analysis. Mathew et al (2013) and Dahal & Hasegawa (2008) also did the analysis on influence of antecedent rainfall on threshold but intensity-antecedent relationship were not built. Tien Bui et al., (2013) applied daily-antecedent rainfall threshold in Vietnam. And Gabet et al (2004) developed intensity-antecedent rainfall threshold in Nepal but the I-A relationship cannot presented by linear relationship.

Physically-based analysis based on slope stability and hydrological condition. The threshold will be defined by modelling which considers soil physical properties, slope features, hydraulic change and other related factors (Capparelli & Tiranti, 2010). Thiebes et al (2014) built a physical model combine hydrology and stability together and put it into EWS of landslides. The physically-based analysis mainly relay on detailed parameters and appropriate model. The simulation of landslide in high elevation mountain area is very complex. No physically-based rainfall threshold has been done in Nepal.

The rainfall indexes used in threshold definition are also different. Daily rainfall forecasting was used by Devi (2014) to make EWS for landslides in India. Rainfall intensity and duration are used in threshold research by Zhou and Tang (2014). Baum (2010) pay more attention in antecedent rainfall, rainfall intensity–duration, and real-time monitoring of soil moisture in EWSs for rainfall-induced shallow landslides and debris flows in America.

An appropriate threshold for EWS is based on a suitable landslide model, trustful landslide parameters (soil character and topology), and rainfall data. There are empirical models and physical models for the estimation of rainfall thresholds. Empirical landslide modelling is based on historical statistic data. Cappare and Versace (2011) explained the application of FLaIR and SUSHI model in EWSs. FLaIR is a hydrological model that based on landslide characters and antecedent rainfall. SUSHI is a complete model that based on Limit Equilibrium Methods. A regional scale model Landslide Hazard Assessment for Situational Awareness (LHASA) has been developed by Kirschbaum, Stanley and Simmons (2015) in Central America and Hispaniola (Kirschbaum, Stanley, & Simmons, 2015). This model takes soil features, rainfall intensity, antecedent rainfall, topography, road network, and distance to fault into consideration. Physical landslide modelling is based on landslide mechanism. Liao et al. (2010) used SLIDE model in their EWS for rainfall triggered landslides, the model mainly based on slope properties, soil properties, and rainfall properties.

STARWARS + PROBSTAB model was developed by van Beek in 2002, the model is consist of a dynamic hydrological model STARWARS and a stability model PROBSTAB. SHALSTAB model was developed by Dietrich (1998) which concentrate on steady-state runoff and infinite slope stability. TRIGRS is developed by Baum et al (2002) to generate stability by calculating pore water pressure and rainfall infiltration. How to choose a proper model should depend on data availability and landslide characters.

The main limitation of the empirical model is the availability and accuracy of historical data. Both historical landslides inventory and antecedent triggering rainfall are needed in empirical modelling, and the quality has a significant influence on the result. There is no open source or another platform that we can get the detail of each landslide, such as the exact date, location, and any antecedent movement. That make it very difficult to build up the empirical model and validate our final result. Limitation of physical modelling also existed. Parameterizing the model over a large area will be very difficult. Data such as soil depth, soil shearing strength, and infiltration are not available in regional scale. In this case, models are not the only limitation. The availability and accuracy of the data are huge problems. Soil properties in Himalaya mountain region are different from normal soil. The gravel content is high because of the colluvial origin. Xu et al., (2011) applied large-scale direct shear test in the field in order to study the shear strength of such soil-rock mixture. Wang (2011) did experimental research on the shear strength of gravel soil. An indoor large-scale direct shear test is used in his study. These studies all focus on gravel mixed soil from Sichuan China similar with Nepal that suffered from earthquake events.

Rainfall is a very important factor in rainfall-induced shallow landslides. There are not so many rainfall stations in Nepal, especially near our study area. These stations mainly use manually record and that provide uncertainty. Satellite rainfall data are available but the resolution is very large. Using satellite rainfall data in EWS is not new, satellite data based EWSs for rainfall-related hazards such as drought and flood had been designed for the last decades. Tropical Rainfall Measuring Mission (TRMM) has been widely used in EWSs. Liao et al (2010) made a prototype EWS using TRMM rainfall data in Indonesia. The satellite-based precipitation monitoring system and a precipitation forecasting model are involved in the EWS. There are already studies of deriving precipitation data from TRMM data in Nepal (Barros et al., 2000; Bookhagen & Burbank, 2006). Barros compared the TRMM-derived data with rain gauge data, found that satellite data shows a better accuracy in lower altitude. Bookhagen used TRMM to find out the influence on rainfall of topography and relief. There is also a new generation satellite based source Global Precipitation Measurement (GPM), which was put forwards at 2007 (Smith et al., 2007) and put into use in April, 2015. Gaona et al (2016) did the evaluation of GPM rainfall over the Netherlands. Oliveira et al (2016) made the analysis using GPM data over central amazon region. No research or validation has been done near Himalaya area.

#### **1.4. Objectives**

General objective:

Development of rainfall thresholds as a component of a regional Landslide Early Warning System using satellite-derived rainfall in combination with physically-based landslide initiation modelling for a test area in Nepal.

Specific objectives

1. Compare data from rainfall stations and satellite derived rainfall products as model input.
  - ✧ What are the advantages and disadvantages of each data source?
  - ✧ What the correlations between the different data source?
  - ✧ Which data is the most appropriate input for physically-based modelling
2. Parameterizing a physically-based model with data from a data scarce environment. How to simulate the soil depth and how to evaluate the result?
  - ✧ How to parameterize with limited information?

- ◇ How to define the initial condition?
- 3. Adapt an existing physically-based landslide initiation model reflecting the poor data availability.
  - ◇ What are the main mechanisms and factors that play a role in the generation of landslides in the study area?
  - ◇ What are the hydrological and geomechanical assumptions for the physically-based model?
  - ◇ How to evaluate the model when there is not enough historical data?
- 4. Define appropriate rainfall thresholds based on the physically-based modelling
  - ◇ How to build rainfall-landslide relationship model?
  - ◇ How to validate the results with limited landslide data?
  - ◇ How to deal with overprediction?

## 1.5. Methodology

The methodology are consist of three phase: parameterization, modelling, and threshold definition. The flow chart of methodology is shown in Figure 1-1.

### Fieldwork

The main purpose of field work is to collect information about landslide to complete the EWS, such as landslide type, soil parameters, geomorphology, land use/cover, etc.

- Go to Rasuwa, Nepal, investigate the existing landslides in study area. Find out the dominating landslide type and its characteristics.
- Do some simple survey in some representative landslides, record the related data. Using these data to find out the influence of rainfall and mechanism of landslides.
- Interview local people or use questionnaire to get information of landslides, including landslide location, landslide occurrence time, and relation with rainfall.
- Take soil samples from landslide area. Soil physical parameters such as porosity, density, grain content, and shearing strength can be obtained through indoor experiments.

### Landslide inventory data

The landslide inventory data mainly consist of landslide location, landslide type, and date of occurrence. This data should come from different sources: existing inventories, image interpretation, fieldwork, community based interview (asking local people), etc. The existing inventories and image interpretation can locate the landslide in regional map but cannot reveal the landslide type and occurrence date. Fieldwork and interview can acquire local scale detail landslide information. But the accuracy of data from the interview cannot be ensured. There methods will be complementary in the data acquisition.

### Soil and hydrological parameters:

The quality of these parameters will have significant influence on the final result. There are three main sources of landslide parameters. The first source will be collect from field, such as soil type, soil depth, land cover/use, etc. The second type of the parameter like shearing strength, porosity, unit weight, and water conductivity will need further study of laboratory tests. The rest of the parameters such as infiltration capacity, canopy storage, throughfall ratio, air entry value, soil water retention curve, matric suction, evapotranspiration, and tortuosity of river, they will be calculated based on available data or acquired form literature.

### Rainfall data

TRMM had been widely used in rainfall related hazards monitoring and early warning. GPM has advantages of high spatial resolution and temporal resolution. Which data will be used in this project is still an open question. Shallow landslides have close connection with current rainfall intensity and quick response. Deep landslides have more connection with antecedent rainfall, so the response is relatively slow. Also the infiltration will have influence on response. The different rainfall-landslide pattern will affect the EWS model. How to choose rainfall factors will be determined based on landslide conditions in study area. Rainfall station data will be used in RS rainfall data validation. The data were managed by Department of Hydrology and Meteorology

### **Establish the precipitation-landslide model**

Based on the key factors above, precipitation-landslide model could be established. Field data, RS based data, and satellite rainfall data are the three main input of the model. All the landslide related parameters like soil depth and water table should be converted into maps. Interpolation and other methods will be used in data processing. All the RS maps should use same coordinate and convert into same resolution. In order to define appropriate rainfall threshold, average daily rainfall data will be used in the modelling. In monsoon season, continuous heavy rainfall will keep soil in high saturated condition. The initial condition such as soil moisture and water table will be different from the field observation. These initial condition of the physical model will be calculated outside the STARWARS + PROBSTAB model and based on historical rainfall data, topography, and soil hydraulic characteristics.

STARWARS is a dynamic hydrological model, soil hydraulic features, slope characteristics, and rainfall will be taken into consideration. This model was originally developed to analyze vegetation influence on hydrology, so the land cover/use and vegetation features are also important parameters in the modelling. STARWARS model stimulate the water condition change of unsaturated soil, suction, infiltration, and percolation are all involved in the modelling. 3-hourly updated water table and soil moisture data are the output of STARWARS, and also will be the input data of PROBSTAB model.

PROBSTAB is landslide stability model based on the infinite slope model. Take into account hydrological data and soil shearing strength, soil depth, slope angle, and root condition, PROBSTAB is able to calculate the landslide stability and failure probability. There are many detail parameters not available in the modelling such as potential evapotranspiration, matric suction of soil, air entry value, etc. Assumptions will be made by using value calculated from other parameters or literature value.

### **Threshold definition**

A dynamic stability map will be the output of the physical model. Complex topography and slope characteristics make different specific spot has different response to a certain rainfall condition. Multiple threshold will be defined to connect unstable area directly with rainfall intensity.

### **Validation**

The validation of the physical model should be based on the historical landslide data. Compare the landslide susceptibility map, historical landslide inventory, historical rainfall data, and field observed data. Check if this area is defined as possible landslide area. The result can be helpful in model improvement.

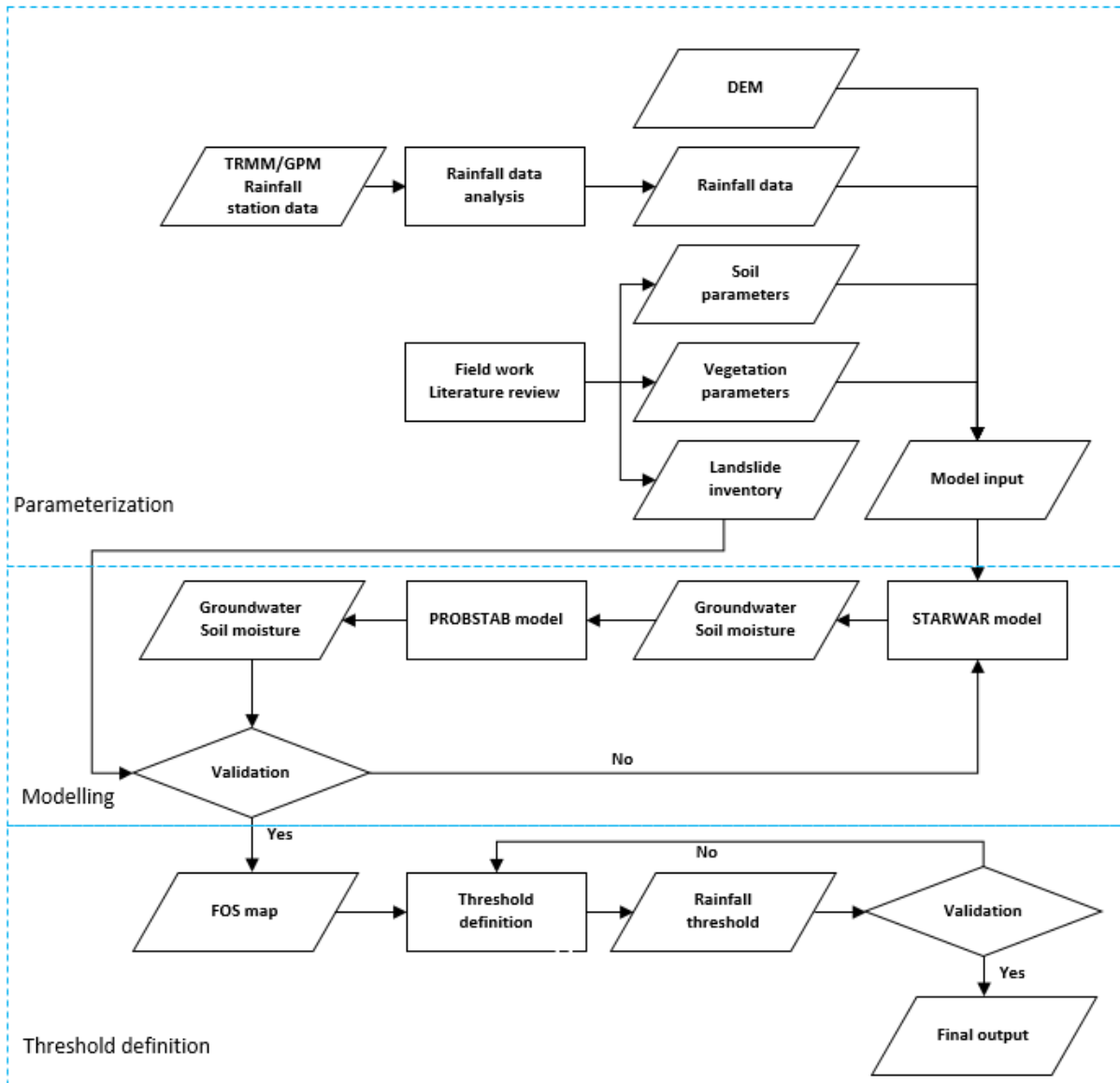


Figure 1-1 Flow chart of methodology

## 2. STUDY AREA

### 2.1. Location and general description

The Rasuwa district is located in the middle north part of Nepal (Figure 2-1), near Himalaya, Elevation varies mainly from 400 to 5000 meters. The test area lies between 27.95° to 28.15° N and 85.13° to 85.35° E, covers about 425 km<sup>2</sup> area, with altitude ranging from 579 to 4043 meters. More than 70% area in Rasuwa have slopes with steepness over 20°.

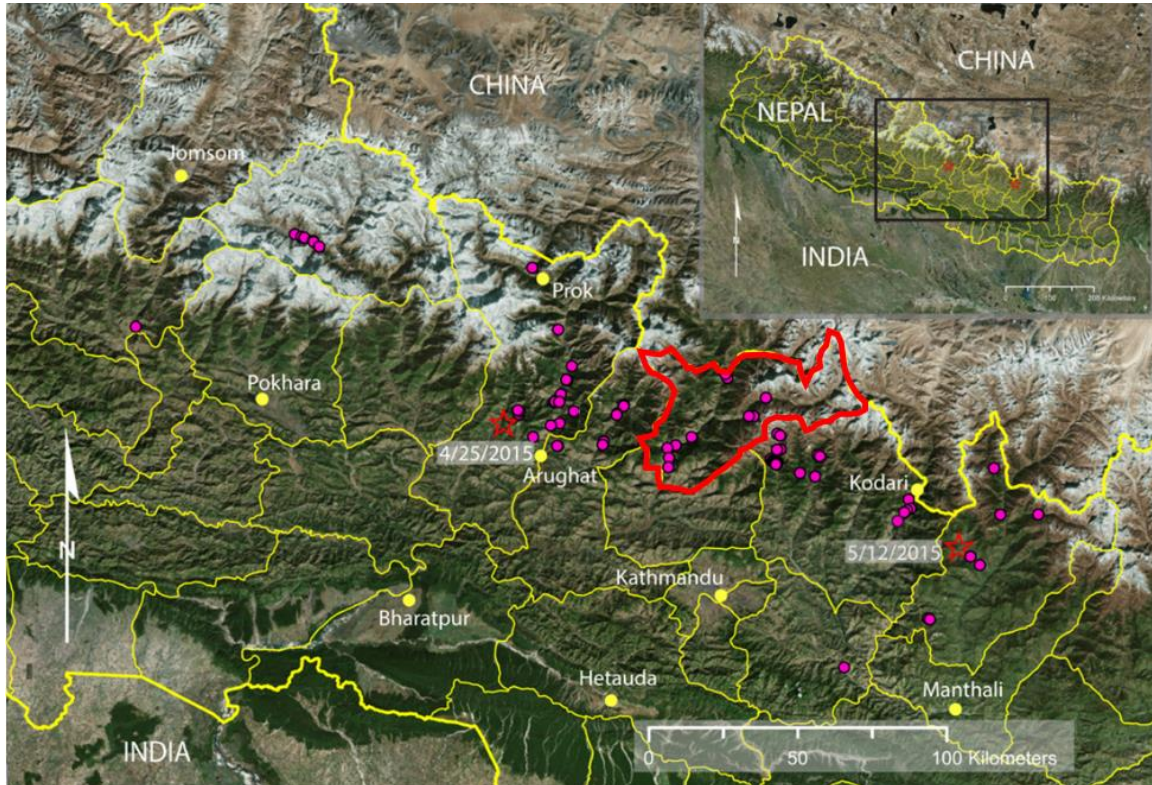


Figure 2-1 Valley-blocking landslides (Pink spot) after 2015 earthquake in Nepal, Rasuwa in red boundary (Collins & Jibson, 2015).

The most important economic income in this area is agriculture. Road cut, farming, and deforestation all create unstable slopes, especially along the rivers and highway towards Chinese border. The infrastructure in this area is not developed and several areas are exposed to shallow landslides.

Langtang National park is located in north-east part of Rasuwa and the largest debris avalanche destroyed the whole Langtang Village after 2015 earthquake (Collins & Jibson, 2015). There are several hydropower station projects along the Trishuli River that were under construction in 2015. The earthquake and co-seismic hazards destroyed their prefabricated houses, and according to the local people several workers lost their lives (Figure 2-2 a, b). The projects did not restart till the field work.





Figure 2-2 a, b. The houses and cars destroyed by co-seismic landslides

## 2.2. Climate

Rasuwa area has a special climate that closely connected with elevation. Because the climate in Nepal is significantly influenced by Indian Monsoon (Figure 2-2). During June to September, the summer monsoon brings warm and moist air from the south-east. The water vapor is blocked by high elevation mountains and become large amounts of rainfall.

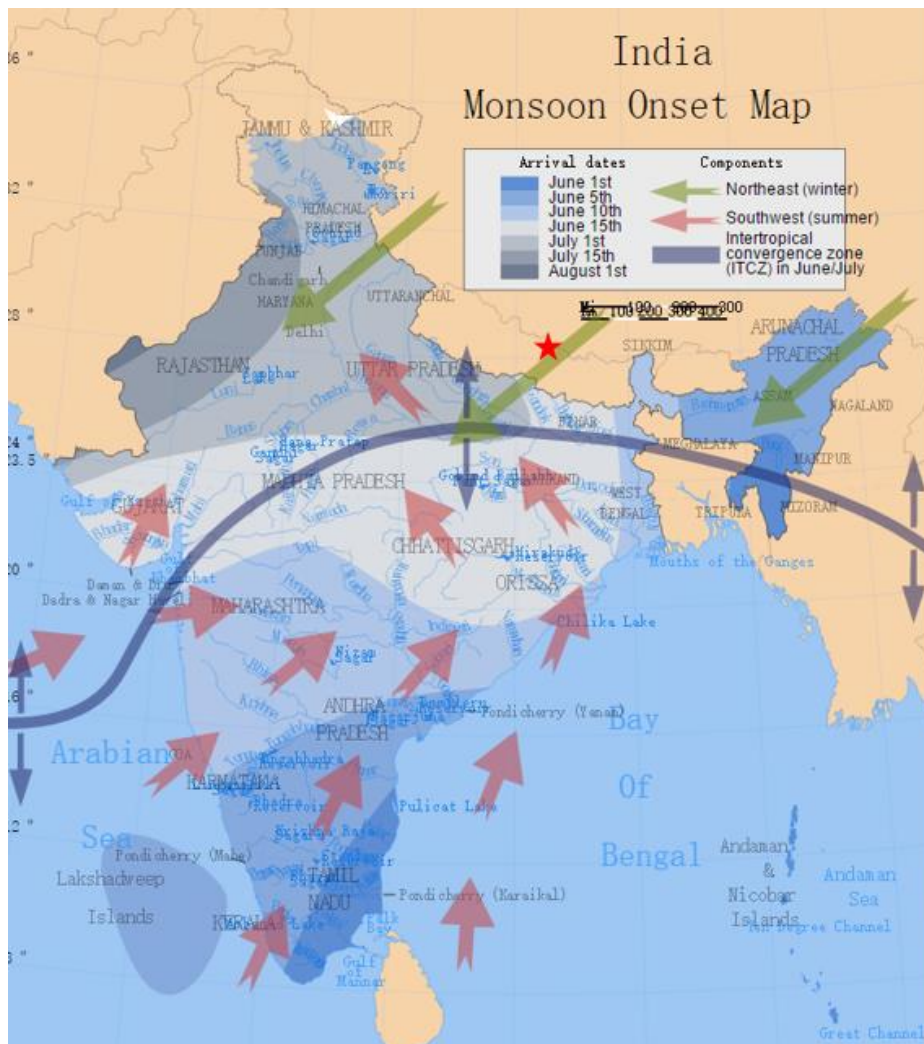


Figure 2-3 The India Monsoon Onset Map (Burroughs, 1999) red star represent Rasuwa area



## 2.4. Field work

### 2.4.1. Preparation

Field work had been conducted during 27th September to 27th October. Before the field work the Nepal working group preparation included the following tasks: Imagine interpretation such as landslide mapping and land use mapping have been done based on Google earth images. Landslide maps are used in identifying the new landslides triggered by rainfall. The Google earth images were taken after the earthquake and before the monsoon season, the new landslide mapping covered landslides both triggered by 2015 and 2016 monsoon. However, they can be distinguished by the freshness of the surface and the vegetation condition. All the interpolated maps were calibrated during the field work.

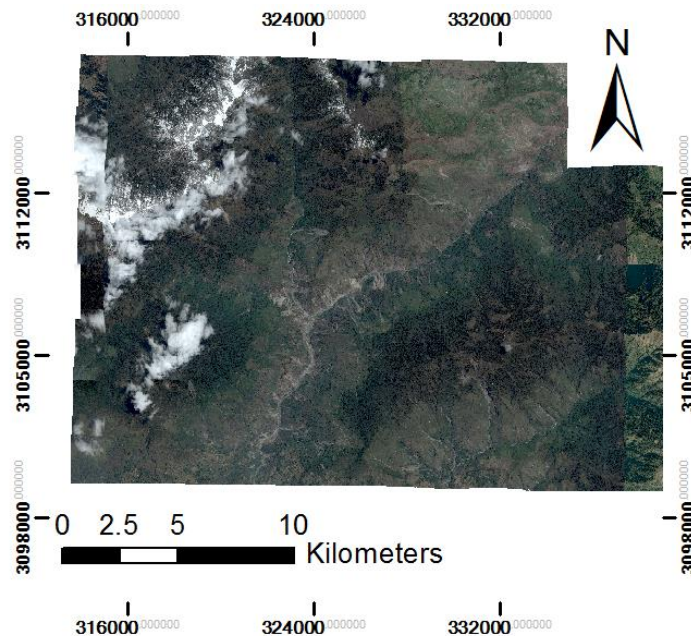


Figure 2-7 Mosaic base map of study area (source: Google earth)

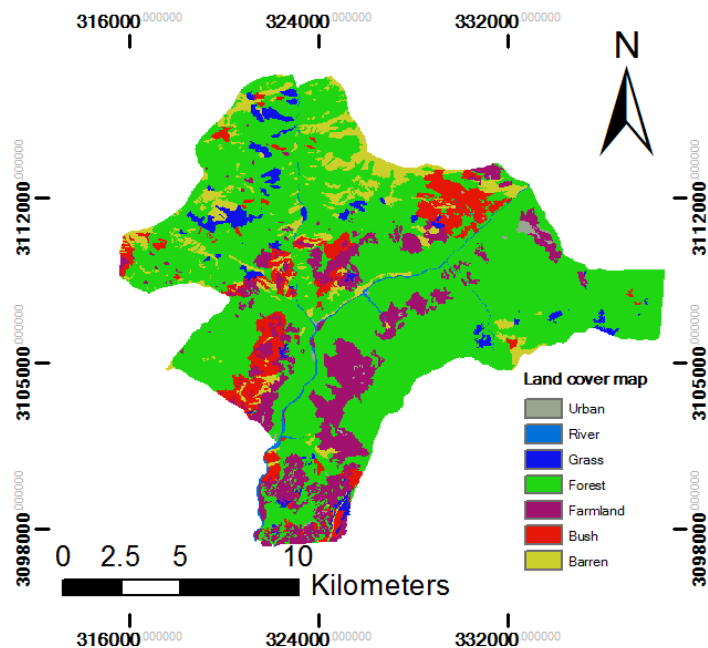


Figure 2-8 Land cover map of study area based on interpretation and field investigation (source: field group work)

### 2.4.2. Field investigation

The open source data of Rasuwa area are still not available. The physically-based model needs detailed information in regional scale. The main objective of the field investigation is to fill the missing data. It is impossible to get all the data within 1 month. The investigation will focus on landslide information and soil information because of the limited time and source.

The field investigation calibrated the landslide mapping based on Google map image (Figure 2-9, Figure 2-10). Based on the freshness and vegetation condition in the slip surface, newly rainfall-induced shallow landslides are marked. The calibrated map contains 528 co-seismic landslides and 146 rainfall-induced landslides in the study. And 67 new landslides are triggered or reactivated by rainfall during 2016 monsoon season.

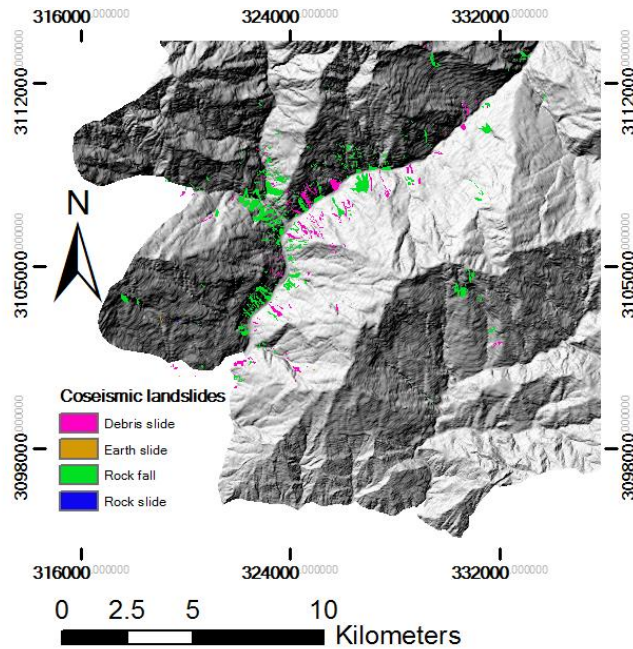


Figure 2-9 Co-seismic landslide mapping based on Google earth and field group investigation

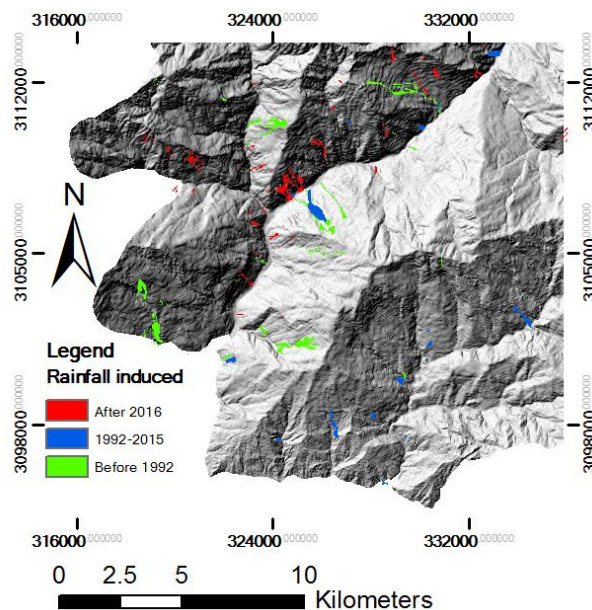


Figure 2-10 Rainfall-induced landslide mapping based on Google earth and field group investigation

Soil type, soil depth, and other soil parameter maps are important inputs of the physically-based model. The soil depth data can be stimulate based on DEM, but still need validation and calibration to make sure the data quality. Based on the observation of scarps and outcrops, 14 soil depth points are recorded during the field work (Figure 2-11). The data include location, deposit characteristics, and estimated soil depth. Soil depth are measured based on the field observation. The outcrops and landslide scarps all reveals the soil depth, otherwise the soil depth will be measured by estimation. These data will be used in calibration of the soil depth model. The table of soil depth is in Appendix 1.

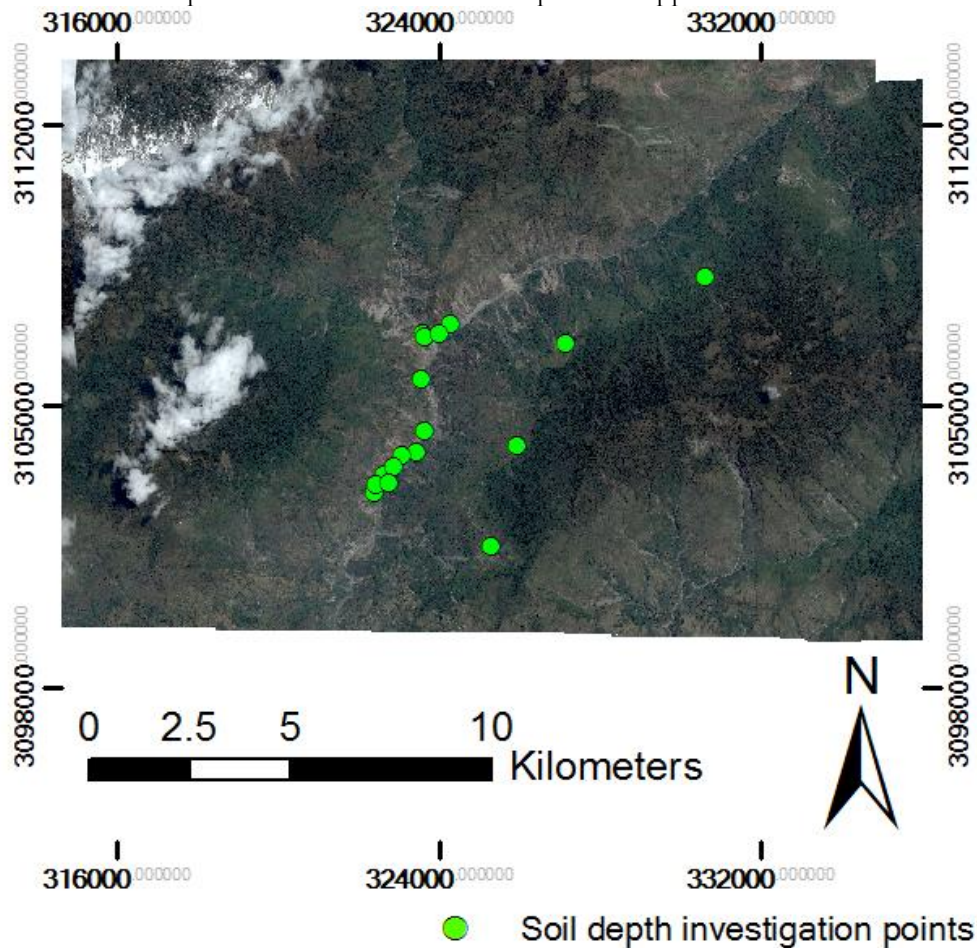


Figure 2-11 Soil depth investigation points

Soils in this area have special features that high gravel content, low clay content, and irregular grain shape. These features are mainly because the soils in this area are developed from colluvial deposit by weathering and water. The soil characteristics between different locations did not vary significantly. And limited by roads condition and time, it is impossible to collect detailed soil type in this region. United soil type will be considered in this study.

#### 2.4.3. Soil sample and soil testing

Soil mechanics factors are also not available. Because the limitation of time, 6 soil samples are taken in different location and different depth. With the help of Tribhuvan University, all the indoor tests are conducted in the laboratory of Central Department of Environmental Science. Grain size test can be used to analysis the component of soil particles and then to determine the parameters. The water conductivity tests are done to provide the Ksat. Soil related parameters will be discussed in Chapter 4. Soil sample information table is shown in Appendix 1. Soil test result is shown in Appendix 2.

## 3. RAINFALL DATA ANALYSIS

### 3.1. Introduction

TRMM is not the only available satellite rainfall data. There is also a new generation satellite-based source Global Precipitation Measurement (GPM), which was put into use in April 2015. GPM data provide better temporal and spatial resolution data (maxima 0.1° and 0.5h). But it is so new that very limited research have been done on it. Validation should be done to verify that whether the data is reliable. Also, GPM has another limitation that data only available since April 2015. Rainfall station data are provided by the Department of Hydrology and Meteorology from 2013 to 2015. Because of the missing data and unknown uncertainty, no data among these three type can be considered as 100 percent trustful. The comparison will be done to identify the quality of the data.

The main objective of this rainfall data analysis is to find out the most appropriate rainfall input for the physical model. Pearson correlation coefficient and significance will be calculated.

### 3.2. Daily rainfall

#### 3.2.1. Rainfall station data

In total data from 7 rainfall stations are used, of which 5 are in or near Rasuwa region (Figure 3-1), while the other 2 are near Kathmandu. Of the 22 Automatic Weather stations in Nepal (Karki, 2000), none is located in or close to the Rasuwa district. All rainfall data used are recorded by traditional manual observation technique. All station datasets consist missing data, noted as NaN, even more than 100 days per year. The period of measurement is from 2013 to 2015, the 2016 data is not available. Details on the rainfall stations can be found in Table 3-1. Examples of rainfall station data are shown in Appendix 4.

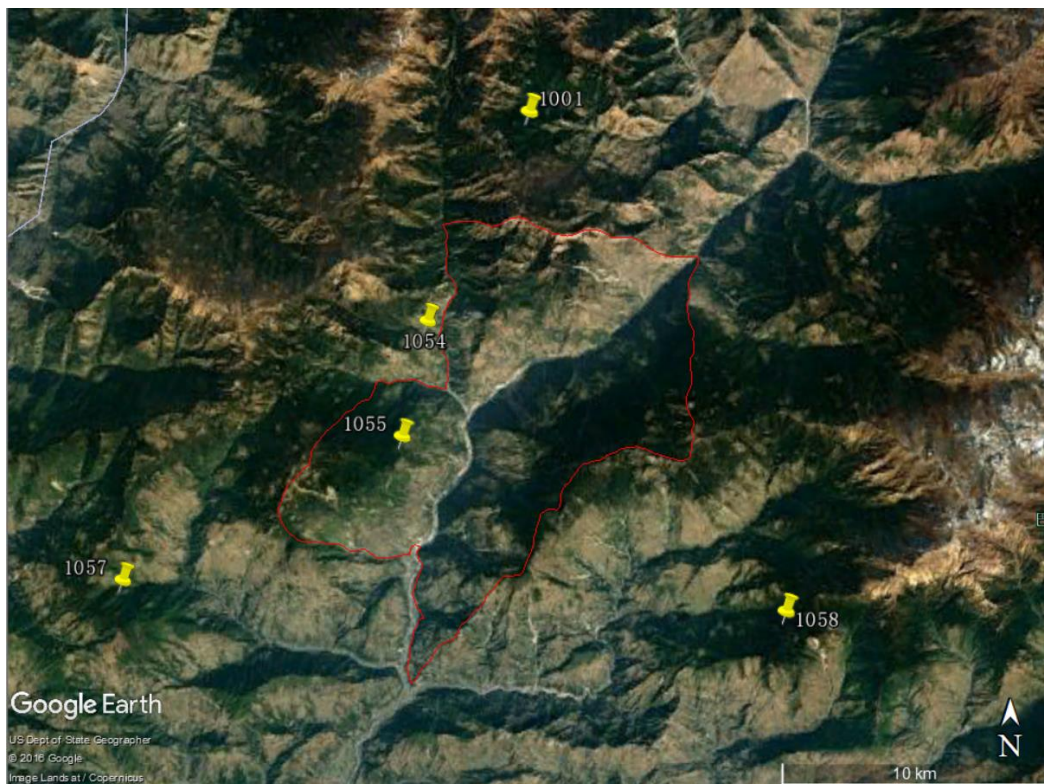


Figure 3-1 Location of rainfall stations near study area (source: Google earth)

Table 3-1 Rainfall stations information

Station No	Aspect [°]	Elevation [m]	Steepness [°]	latitude [°]	longitude [°]	Precipitation Sum(2015) [mm]	Precipitation daily max (2015) [mm]	Nr of NaN (2013-2015)
1058	305	2468	22-27	28.00	85.33	2573	102	290
1057	58	2052	25-33	28.01	85.07	1800	87	35
1055	99	2610	24-33	28.06	85.18	1140	53	60
1054	58	2054	30-36	28.1	85.19	589	35	274
1001	14	3130	17-26	28.17	85.23	427	27	188
1017	309	1800	22-25	27.52	85.34	1724	5	18
1004	60	1200	30-32	27.55	85.1	1479	4	43

### 3.2.2. Correlation analysis

This Table.3-2 shows the Pearson correlation coefficient (PCC) and significance (sig) between different rainfall stations. The PCC value shows the linear dependence of these two group data, the significance (sig) represent the correlation between two stations, sig < 0.05 means these two group of value have more than 95% present possibility of high correlation. In the table above, station 1001 have very low sig value with 1054, 1055, and 1058 which means they have a high possibility of correlation but the PCC values are not very high, which means they do not have a good linear relationship. Station 1001, 1054, 1057, 1055, and 1058 are all near the study area, they all influenced by the almost the same weather condition, so their data should have correlation. But their significances are not very low, which means their correlation may not very good. This inconsistency shows the uncertainty of the rainfall station data.

Table 3-2 Pearson correlation coefficient and significant of rainfall stations

Station No	Index	1001	1054	1057	1055	1058	1004	1017
1001	PCC	1.00	0.27	0.11	0.45	0.50	0.17	0.13
1001	sig	--	0.01	0.25	0.00	0.00	0.07	0.17
1054	PCC	0.27	1.00	0.14	0.14	0.05	0.14	0.24
1054	sig	0.01	--	0.16	0.17	0.63	0.18	0.02
1057	PCC	0.11	0.14	1.00	0.03	0.28	0.00	0.24
1057	sig	0.25	0.16	--	0.71	0.00	1.00	0.01
1055	PCC	0.45	0.14	0.03	1.00	0.31	0.19	0.27
1055	sig	0.00	0.17	0.71	--	0.00	0.05	0.00
1058	PCC	0.50	0.05	0.28	0.31	1.00	0.20	0.20
1058	sig	0.00	0.63	0.00	0.00	--	0.04	0.03
1004	PCC	0.17	0.14	0.00	0.19	0.20	1.00	0.44
1004	sig	0.07	0.18	1.00	0.05	0.04	--	0.00
1017	PCC	0.13	0.24	0.24	0.27	0.20	0.44	1.00
1017	sig	0.17	0.02	0.01	0.00	0.03	0.00	--

### 3.2.3. Conclusion

The precipitation in mountain area will be influenced by cloud, elevation, leeward/windward, and slope steepness. The Table reveals that the annual total and maximum daily precipitation (in Table 3-1 per station) did not show a clear relationship with elevation, aspect, and steepness. But it is clearly revealed that in figure 3-2 and figure 3-3 the precipitation shows a clear gradient with small values in the north to larger values in the south, following the pronounced monsoon wind direction (Figure 2-3). From east to west, the trend is disturbed by station 1058. And the reason of high precipitation in 1058 is located near the peak of the mountain. This area will have higher precipitation than other rain shadow part.

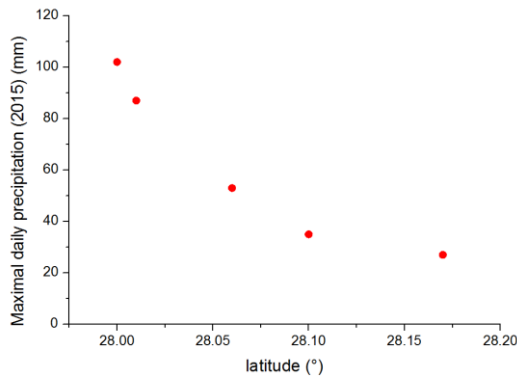


Figure 3-2 Correlation between latitude and maximal daily precipitation of 2015

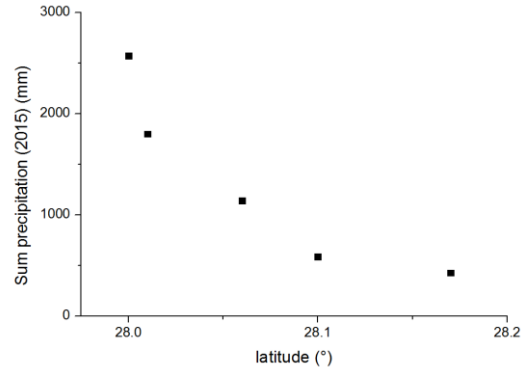


Figure 3-3 Correlation between latitude and sum precipitation of 2015

Take station 1017 which has the least missing data as an example, plot the scatter between 1004 (near 1017) and 1001 (far from 1017) (Figure 3-4, Figure 3-5).

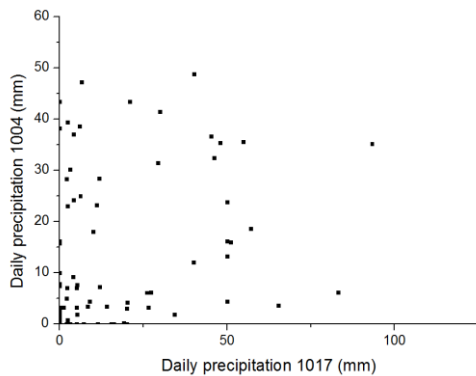


Figure 3-4 Scatter between station 1017 and 1004

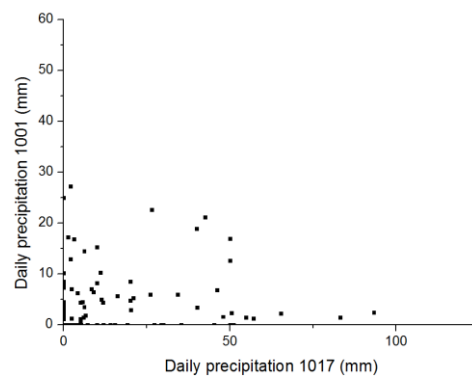


Figure 3-5 Scatter between station 1017 and 1001

In the Table 3-2 station 1004 has the highest PCC value with 1017 which means they have the best linear relationship among all the stations. They all located near Kathmandu and in flat areas. While 1001 is far from 1007 and in high elevation, the linear relationship is not good. A lot of scatters are in the X-axis and Y-axis which means the rainfall pattern in these two stations are not the same. The low sig values in the Table 3-2 reveal that the rainfall data have correlation but the very low PCC values show that there linear relationship is not satisfied. This is mainly because the rainfall in mountain area is very complex, the spatial distribution of rainfall involve more factors than simple location and elevation.



### 3.3. Satellite based precipitation comparison

#### 3.3.1. TRMM and GPM data

The information of satellite rainfall product is shown in Table 3-3.

Table 3-3 information of satellite rainfall products (NASA website)

Name	algorithm	Temporal resolution	Spatial resolution	Latency	Time span
TRMM	3B42 RT	Daily	0.25°	8 hour	March 2000 to present
GPM	IMREG	Daily	0.1°	6 hour	April 2015 to present

There is only 1 pixel near study area (Figure 3-6) because of the low resolution. While 9 pixels covering the study area are analyzed in GPM data (Figure 3-7). The GPM data only available after April 2015, however, the monsoon season is the focus. Data from June to September are used in the analysis. Examples of GPM satellite rainfall data are shown in Appendix 5.

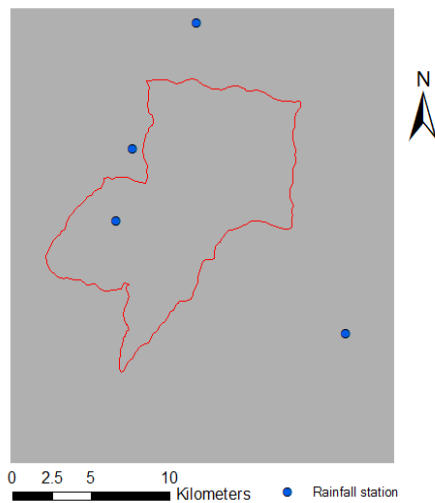


Figure 3-6 Pixel of TRMM data near study area

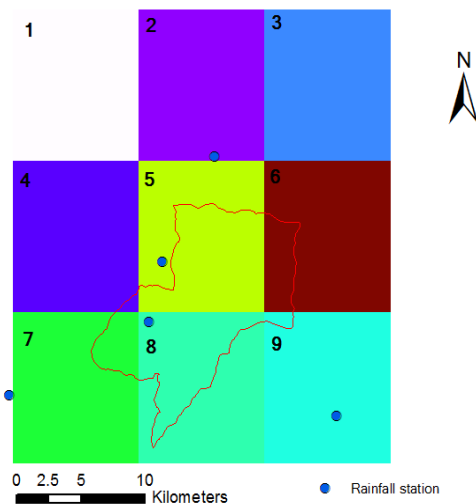


Figure 3-7 Pixels of GPM data near study area

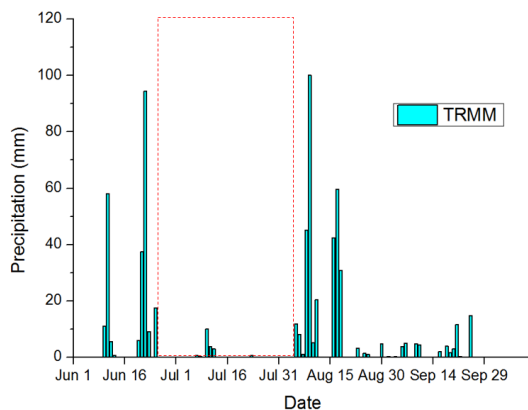


Figure 3-8 The daily precipitation derived from TRMM (2015 monsoon)

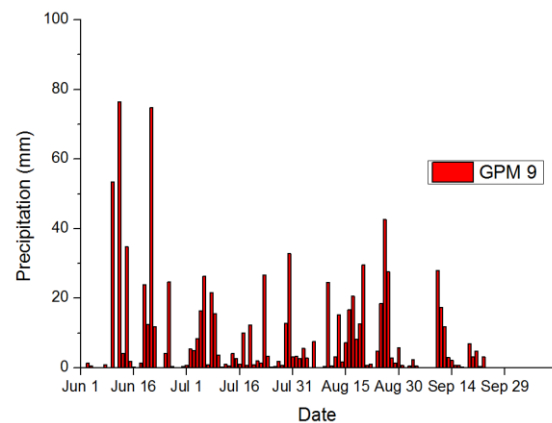


Figure 3-9 The daily precipitation derived from GPM pixel 9 (2015 monsoon)

Compare the daily precipitation during monsoon season (Figure 3-8, Figure 3-9), there is a significant gap between June 20<sup>th</sup> and Aug 5<sup>th</sup>. During the monsoon season, over 30 days without any heavy rain is

impossible in the study area. Both GPM data and rainfall station data show that there is intense precipitation during this time. There are two possible reasons for the gap, first one is because the TRMM data have low resolution and our study area is just in the boundary of middle Himalaya (elevation about 3000m to 4000m) and great Himalaya (average elevation > 6000m). In great Himalaya part, the precipitation is quite low because of the extremely high elevation. And the pixel value of TRMM data is the average value of whole pixel area, the algorithm of TRMM may put more weight in these no rainfall part. Another possible reason is there are some technic problems in sensors, but there is no explanation in NASA website.

### 3.3.2. Correlation analysis

The correlation analysis calculation is shown in Table 3-4.

Table 3-4 PCC and sig between GPM pixel 1 to 9 and TRMM data

		1	2	3	4	5	6	7	8	9	TRMM
1	PCC	1.00	0.96	0.87	0.91	0.90	0.81	0.77	0.78	0.72	0.09
1	sig	--	0.00	0.00	0.00	0.00	0.00	0.00	0.00	0.00	0.32
2	PCC	0.96	1.00	0.92	0.90	0.94	0.85	0.76	0.79	0.71	0.10
2	sig	0.00	--	0.00	0.00	0.00	0.00	0.00	0.00	0.00	0.26
3	PCC	0.87	0.92	1.00	0.80	0.86	0.94	0.72	0.78	0.75	0.08
3	sig	0.00	0.00	--	0.00	0.00	0.00	0.00	0.00	0.00	0.38
4	PCC	0.91	0.90	0.80	1.00	0.97	0.85	0.92	0.92	0.80	0.18
4	sig	0.00	0.00	0.00	--	0.00	0.00	0.00	0.00	0.00	0.05
5	PCC	0.90	0.94	0.86	0.97	1.00	0.90	0.90	0.92	0.80	0.16
5	sig	0.00	0.00	0.00	0.00	--	0.00	0.00	0.00	0.00	0.07
6	PCC	0.81	0.85	0.94	0.85	0.90	1.00	0.84	0.89	0.87	0.11
6	sig	0.00	0.00	0.00	0.00	0.00	--	0.00	0.00	0.00	0.24
7	PCC	0.77	0.76	0.72	0.92	0.90	0.84	1.00	0.98	0.90	0.19
7	sig	0.00	0.00	0.00	0.00	0.00	0.00	--	0.00	0.00	0.04
8	PCC	0.78	0.79	0.78	0.92	0.92	0.89	0.98	1.00	0.91	0.19
8	sig	0.00	0.00	0.00	0.00	0.00	0.00	0.00	--	0.00	0.03
9	PCC	0.72	0.71	0.75	0.80	0.80	0.87	0.90	0.91	1.00	0.14
9	sig	0.00	0.00	0.00	0.00	0.00	0.00	0.00	0.00	--	0.12
TRMM	PCC	0.09	0.10	0.08	0.18	0.16	0.11	0.19	0.19	0.14	1.00
TRMM	sig	0.32	0.26	0.38	0.05	0.07	0.24	0.04	0.03	0.12	--

Compare the GPM pixel values, the table above shows very low sig and very high PCC values, which means the values of each pixel have high correlation and good linear relationship. Also, we can see from the table, the nearby pixel have higher PCC. If two pixels are far from each other, the linear relationship will get worse, however, the coefficients stay still low value. These are mainly because of the algorithm of GPM product. Compare the GPM and TRMM, the table shows that they have low PCC and high sig. They have neither good linear relationship nor good correlation.

### 3.3.3. Conclusion

Plot the TRMM data with GPM pixel 8 (which has the best correlation with TRMM), the plots are concentrated in X-axis and Y-axis (Figure 3-10). And plot the pixel 8 and pixel 9, they show significant linear relationship (Figure 3-11).

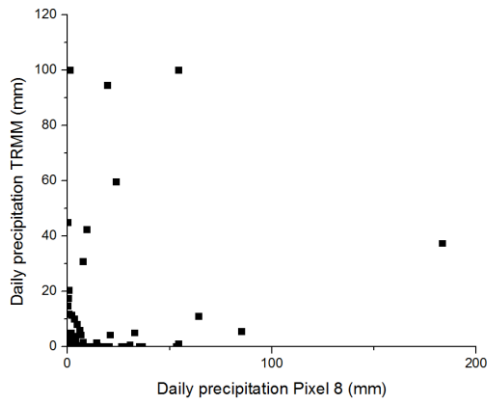


Figure 3-10 Scatter plot between GPM pixel 8 and TRMM

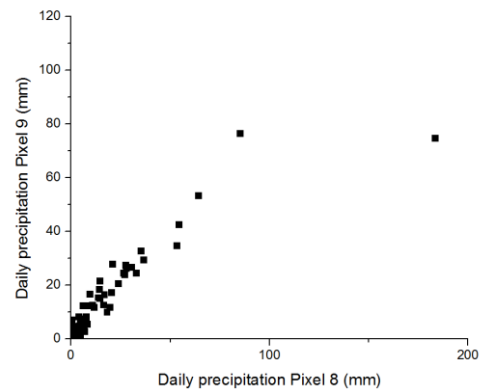


Figure 3-11 Scatter plot between GPM pixel 8 and 9

Different satellite, sensors, and algorithms are the main factors of difference between TRMM and GPM data. And they do not have a simple linear relationship. Consider the resolution, data gap, and correlation, GPM is more suitable in this study.

Table 3-5 Sum rainfall and Max daily rainfall of 2015 monsoon season

Pixel No.	1	2	3	4	5	6	7	8	9
Sum (mm)	313.33	313.12	212.24	541.30	552.10	373.02	697.04	631.30	605.24
Max (mm)	33.83	38.71	30.64	39.76	51.08	36.69	58.31	54.22	42.59

In the GPM pixel data, there is also a trend like rainfall station data, precipitation shows a clear gradient with small values in the north to larger values in the south, following the pronounced monsoon wind direction. This same trend shows the reality of both satellite and station data.

### 3.4. Comparing ground stations with satellite products

The correlation value table between station data and satellite data and table of daily rainfall from all products are in Appendix 3. Compare the rainfall stations with the GPM pixels which cover the stations. Station 1001 (best correlation) is taken as examples. The correlation PCC and sig value are shown in Table.3-6. The scatters of the station of 1-day, 5-day, 10-day, and 15-day accumulated rainfall is shown in Figure 3-12 to Figure 3-15.

Table 3-6 Correlation between station 1001 and GPM pixel 2

		1001	P2
1001	PCC	1.00	0.36
1001	sig	--	0.09
P2	PCC	0.36	1.00
P2	sig	0.09	--

The scatters in Figure 3-12 show very bad correlation, the majority of the points are in or near the axis. These points indicate that when there is rainfall in one data, the other data recorded no rain or less rain. When the time window increase from 1 day to multiple days, the scatters show better and better correlation. One reason for this change is because of the time latency. The GPM data is accumulative data of 3-hour product, while the station data is daily manually recorded. The time latency different will affect both total rainfall and peak value. When the time window increase, the data will get less influence from latency. The red line in the graph is  $y = x$ , the points lower than this line means the 1001 station data has a higher

record than GPM pixel 2 data and vice versa. When the time window increase, the scatters are gathering to three groups, one group below the red line and two groups above. The reason for these group involves other factors, these factors affect either the rainfall gauge or the satellite algorithm. These influence will lead to overestimation or underestimation of rainfall.

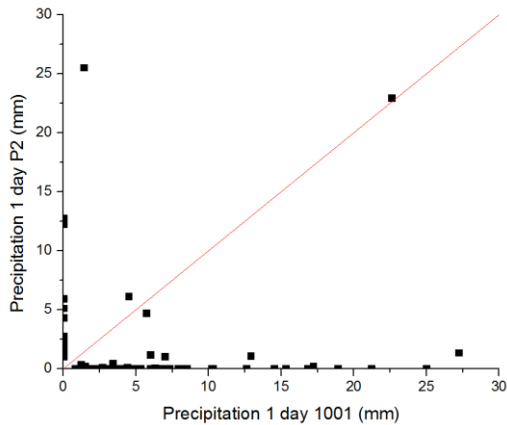


Figure 3-12 Daily precipitation scatter between station 1001 and GPM pixel 2

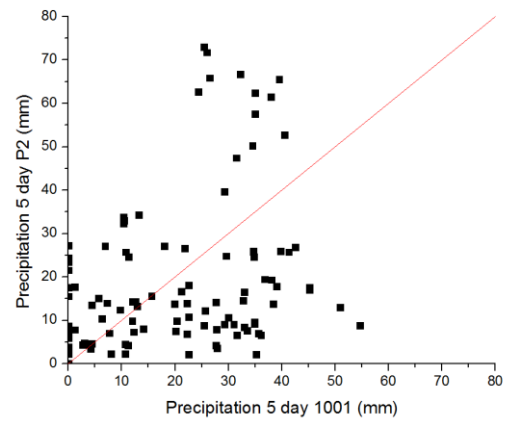


Figure 3-13 5-day precipitation scatter between station 1001 and GPM pixel 2

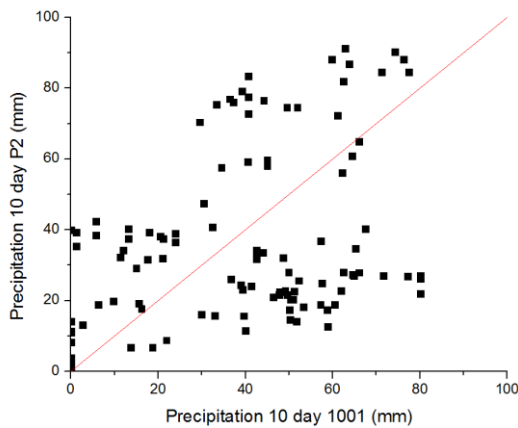


Figure 3-14 10-day precipitation scatter between station 1001 and GPM pixel 2

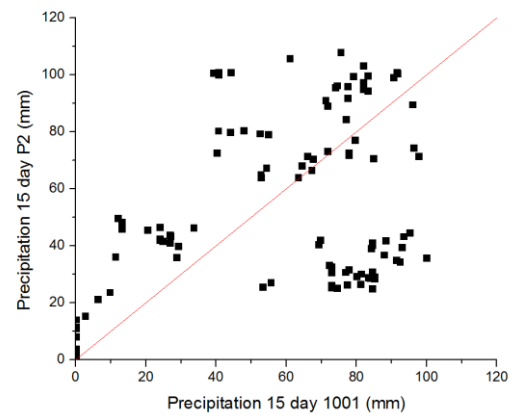


Figure 3-15 15-day precipitation scatter between station 1001 and GPM pixel 2

### 3.5. Conclusion

TRMM data appear to be the worst data in the analysis, low correlation with other product, data gap during monsoon season, and low resolution. The rainfall station data have the problems of missing data and latency. GPM have the best performance in the data analysis but the validation part is still not available. The complex relationship between satellite rainfall data and station data cannot be finished in limited time.

The main objective of this rainfall analysis is to find out the most appropriate rainfall input for the physical model. In order to define the threshold, unit rainfall input will be used in the model. The extreme rainfall events are the focus in the threshold definition. The max value of both station and GPM data can be a good option for input. The GPM data fill the data gaps of station data and this is the easiest way to simplify the difference between two products.

## 4. SOIL DATA ANALYSIS

### 4.1. Introduction

The soil depth and the hydrological and geotechnical soil parameters play a very important role in physically-based landslide modelling. 24 soil related parameters are considered in the STARWARS+PROSTAB model. The soil characteristics in the study area are typical for a high mountain environment, and some are close related to the occurrence of landslides. Old landslide masses exist in many places, which provide fractured rock masses or colluvial soils. Mechanical weathering, due to freeze-thaw cycles, and the high amount of rainfall are responsible for intensive weathering in certain locations. The colluvial soils and weathering soils generally have a high gravel content and large gravel size in the soil sample. These factors make it very difficult to define the geotechnical and hydrological parameters because the normal soil mechanics is sometimes not suitable for gravel mixed soil. A soil characterizing and depth modelling approach and data from literature were considered in parameterizing. Xu et al., (2011) applied large-scale direct shear test in the field in order to study the shear strength of such soil-rock mixture. Wang (2011) did experimental research on the shear strength of gravel soil. An indoor large-scale direct shear test is used in his study. The sample scale is 500mm×400mm and the maximum vertical and horizontal stress are 3.5 Mpa. The large scale sample maintains the characteristics of the gravel soil and reduce the influence of size effect. Yang (2013) also conducted indoor large-scale direct shear tests using samples from Sichuan province that also suffered from catastrophic earthquake events. The result is shown in Table 4-1 and Table 4-2.

Table 4-1 Shear strength of different gravel content (Yang, 2013)

Gravel content (%)	45.94	52.45	55.18	58.84	64.59	68.04
c (kPa)	8.21	15.34	4.14	2.12	4.33	18.45
$\phi$ (°)	40.77	44.22	46.19	46.69	46.56	43.17

Table 4-2 Cohesion under different soil moisture (Yang, 2013)

Soil moisture	0.006	0.08	0.13	0.20	0.24
c (kPa)	15.34	11.07	8.16	3.68	1.45

The study on the vegetation effects on slope stability is not directly the focus of this thesis, but evapotranspiration and root cohesion are crucial factors in physically-based modelling. Zhong (2015) made a research in the Three Gorges Reservoir about the root cohesion of grass. 4 species are tested and the maximal root cohesion is between 3.12-4.90 kPa. Gai (2013) did his Ph.D. research on mechanics of tree root reinforcing soil. The root cohesion is shown in Table 4-3.

Table 4-3 Maxima root cohesion of different root condition (Gai, 2013)

Maxima root cohesion (kPa)		Root diameter		
		3mm	5mm	7mm
Species	Larch	21	43	71
	Pine	29	48	62

Evapotranspiration estimations are made depend on many different factors in different surfaces. Bhat, et al., (2016) did hydrological research in Kashmir Himalaya which has similar characteristics as our study area.

## 4.2. Soil depth model

There are three main sources of soil depth data: existing study in this area, field investigation, and modelling. The existing soil maps are all national scale, they are too coarse for the regional scale modelling. Because of the limited time and extreme field conditions, field soil depth mapping cannot be carried out. One of the best approaches would have been to link soils to Geomorphological mapping, however, this could not be done due to lack of Geomorphological mapping skills. Therefore a soil depth model was considered the easiest way to generate a soil depth map. The field investigation results will be used to validate the model result.

### 4.2.1. Original model

The original soil depth model was developed by Kuriakose et al., (2009). The model stimulate the soil depth based on altitude, slope steepness, wetness, profile curvature, distance to coast, and distance to channels. The model equation is

$$SD = a * d_{coast} + b * d_{channel}/d_{max} + c * S + d * C + e * W + f * DEM/DEM_{max} \quad (1)$$

Where SD is stimulated soil depth (m), a-f are calibration constants (-),  $d_{coast}$  is the distance to the nearest coast (m),  $d_{channel}$  is the distance to channels, S is slope index (-), C is the profile curvature ( $m^{-1}$ ), W is wetness index. In this study, distance to coast, wetness, and the profile curvature are unknown factors that will not be take into consideration. Other calibration constants are shown in Table 4-4.

Table 4-4 Calibration constants of soil depth model

calibration constants	b	c	f
Value	1.5	3	4.5

There are three inputs in this soil depth model, the DEM, slope map, and the drainage channel maps. But the channel map and slope map are calculated based on the pixel direction derived from the DEM map, this model is purely based on the DEM map. From field observations it can be concluded that lower altitudes give deeper soils and areas close to river give deeper soils. The altitude has a higher weight in the modelling in this study because, in Rasuwa area, colluvial deposits are the main source of soil.

Compare the soil depth product with the DEM map, the higher part of the mountain has the lowest soil depth and the deepest soil is in the river part. The graph clearly shows the quality of the DEM has a significant influence on the soil depth result. The DEM used in the model is a 30m DEM (Figure 4-1) derived from 1:50000 topographic map (Survey Department Government of Nepal, 1996). The soil depth product (Figure 4-2) show clear patterns of contour lines.

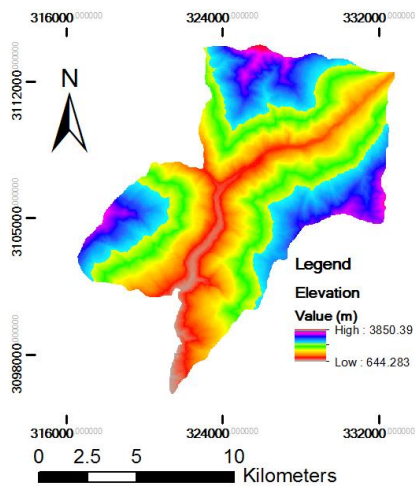


Figure 4-1 DEM map used in the model

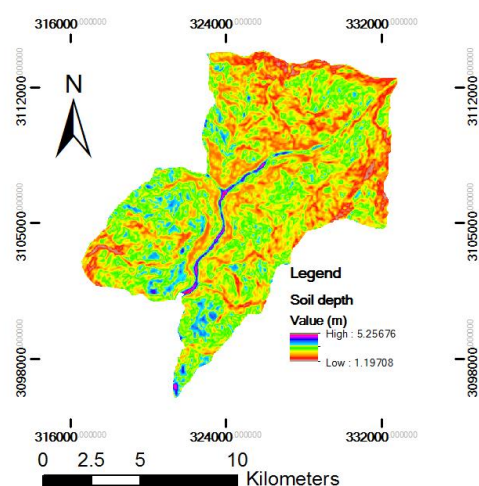


Figure 4-2 Soil depth map of original model

#### 4.2.2. Improved model

The soil depth in Rasuwa is not only based on topography. Human activities have a strong effect on soil depth distribution as well. Different land use and land cover all have an influence on soil depth. For example, farmland is often developed on colluvial deposits, and the farming soil has more organic material, less gravel, smaller gravel size, and thicker soil depth. Also, the historical landslide masses and colluvial deposits also provide extra soil depth. So the original soil depth model based on DEM is not accurate enough and modifications are needed. Extra steps were introduced to improve the soil depth model.

The land use/land cover map was classified into 5 classes (Figure 4-3). And different additional soil depth was given based on field observation. Forest normally grow up in the thick soil, while grass and shrub can grow in any soil depth. The outcrops should have no soil depth but the land cover map did not distinguish outcrops and fresh landslide scarps, they will have a relatively low extra depth.

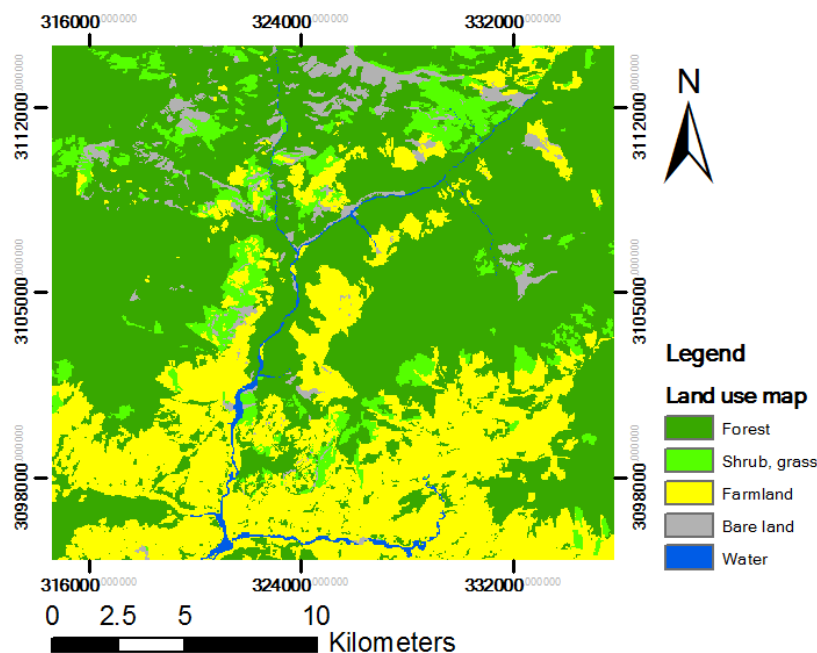


Figure 4-3 Classified land cover map

Table 4-5 Different extra depth of different LULC

Class	Forest	Shrub and grass	Farmland	Bare land	River
Extra depth (m)	2	1	4	0	4

The soil depth also has a close relationship with existing landslide deposits. The landslide mapping is generated based on image interpretation and field investigation. There are mainly two type of landslides in this area: rock fall, rock slides, and debris flow. They have different contributions to soil depth. Rock falls in the study area normally leave large size gravels on the surface (from 10cm to 2m), and the size of the gravel is influenced by the weathering condition of rock masses. The large size gravels did not contribute too much on soil depth while the deposits of antecedent rock falls are turning into gravel soil under the influence of weathering and rainfall. Average value was used in extra soil depth. Debris slides always leave thick deposit on the slope and have higher extra soil depth.



Figure 4-4 Debris slides deposit in Rasuwa

Figure 4-5 Rock fall deposit in Rasuwa

Table 4-6 Different extra depth of different landslides

Class	Rock fall	Debris slides
Extra depth (m)	2	4

The criteria of extra soil depth follow the flow chart (Figure 4-6).

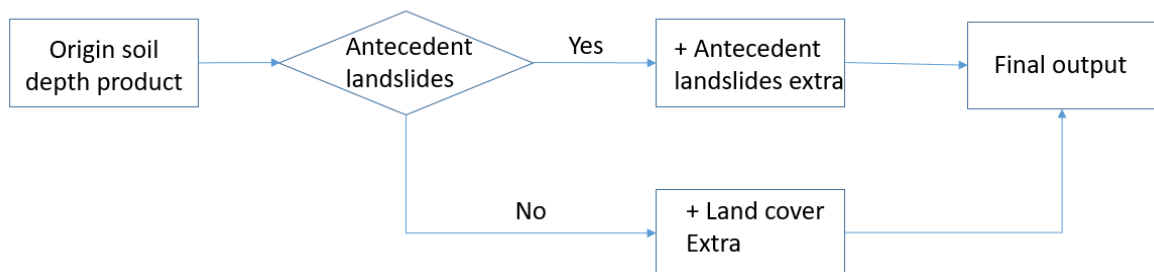


Figure 4-6 Flow chart of extra soil depth



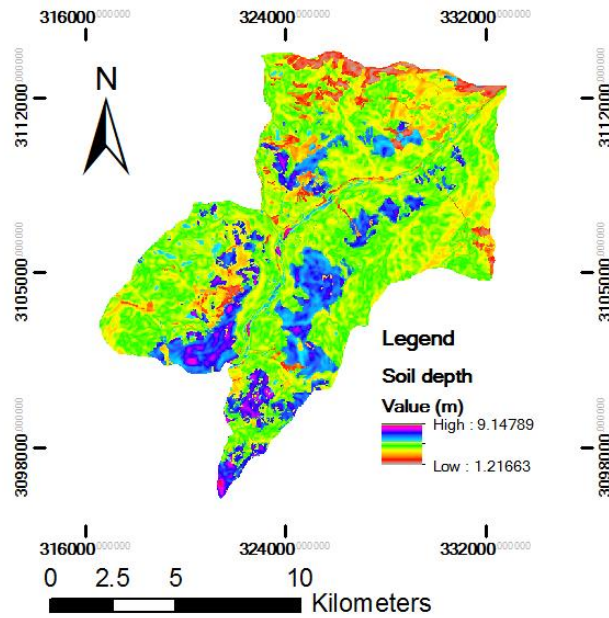


Figure 4-7 Soil depth map of improved model

We can still see from Figure 4-7 that some of the contour line patterns still exist but more factors are involved. Validation is needed to test the model result.

#### 4.2.3. Validation and Conclusion

In order to validate the modified soil depth model, the soil depth measurements from the field were used.

Table 4-7 Field investigation record and model product

Point	D25	D21	D11	D16	D12	D35	Dam	D31	D34
Field data (m)	4	7	5	4	4	8	4	5	10
Original model result (m)	3.03	2.35	2.21	3.4	3.28	3.26	1.98	4.68	3.01
improved model result (m)	5.03	5.35	2.21	5.4	5.28	7.26	3.98	6.68	7
Point	D6	D13	D5	D4	D3	D2	D1	D33	
Field data (m)	5	3	4	3	7	5	4	8	
Original model result (m)	3.02	2.58	3.04	3.06	2.7	2.95	3.73	2.8	
improved model result (m)	5.01	4.58	5.04	5.06	4.7	4.9	5.7	6.8	

Table 4-8 Correlation analysis of soil depth model

		Original model	Improved model
Field data	PCC	-0.07	0.54
	Sig	0.78	0.02

Soil depth data are derived from the maps. The correlation between model and field investigation were calculated (Table 4-8). Before the modification, the model result had a negative Pearson correlation coefficient (PCC) value and very high significance, indicating that they do not have a significant relationship. While after adding the extra soil depth, the significance decreased from 0.78 to 0.02 and the PCC value increased from negative to 0.54. The scatters (Figure 4-8, Figure 4-9) between model result and field data clearly show that the modified model has a better performance than the original one in this case.

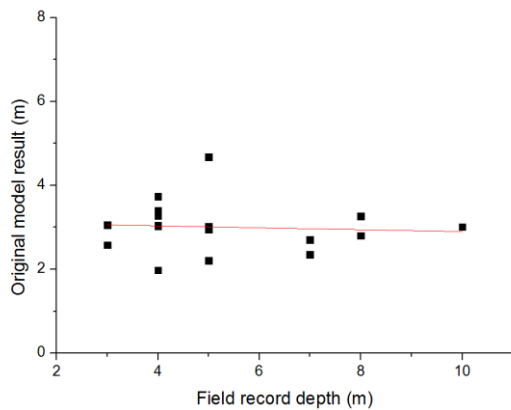


Figure 4-8 Scatters of original soil depth model and field data

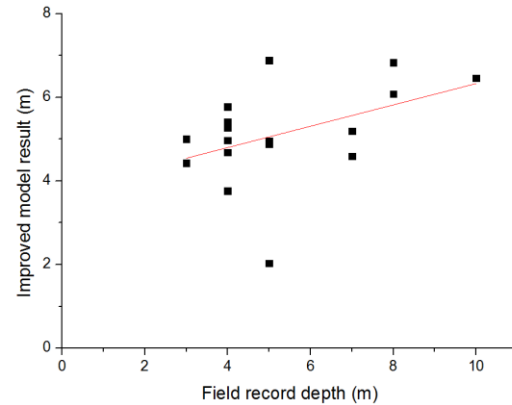


Figure 4-9 Scatters if improved soil depth model and field data

### 4.3. Soil related parameters

The soil related parameters also come from three sources: soil tests, soil characteristic model, and literature values. Seven soil samples were taken in different locations in the study area. Grain size and water conductivity tests were done with the help of Tribhuvan University. The test result are shown in Appendix 2. But these tests are not detailed enough to provide all the soil related input. Saxton (2006) developed a soil water characteristic model (Figure 4-10). Based on field tests, several parameters can be estimated. Also, literature will be considered in parameterization.

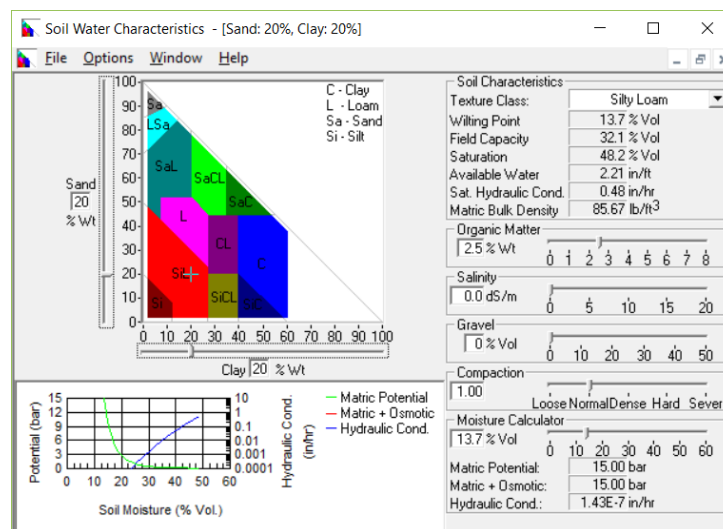


Figure 4-10 Soil water characteristics model

#### 4.3.1. Shear strength

The gravel mixed soil mechanics differs from normal soils, and small-scale laboratory test cannot provide the accurate parameters like shear strength. Large scale field tests have been done by Wang (2011) and Yang (2013), the literature value will be used as input in this model. The internal friction angle values from Yang's (2011) test lie between 40-46°, and values from Wang's (2013) test lie between 20-40°. In Yang's (2011) test, the samples have larger gravel content (46%-68%), and in study area the gravel content derived from test lie between 38-50%.

the gravels in the study area have very sharp edges and irregular shapes and this character make the soil have more friction between grains.  $35^\circ$  is taken as the input for the model.

Soils containing more than 50% gravel are normally considered to be without cohesion between grains. In Yang's (2013) test, the samples with 68% gravel content have cohesion results ranging from 3.17 to 18.45 KPa under different soil moisture (Table 4-2). A linear relationship was obtained between cohesion and soil moisture (Figure 4-11).

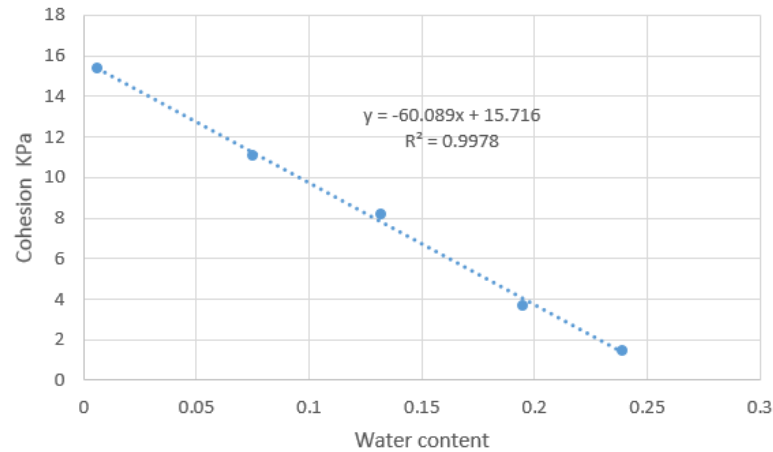


Figure 4-11 Curve of cohesion and water content

#### 4.3.2. Hydrology parameters

Hydraulic conductivity is influenced by porosity, compactness, and vegetation. In this case, vegetation is the most comparable factor. Historical landslides also have larger porosity, and Ksat should be higher. The Ksat values from soil tests and soil water characteristic model are shown in Table 4-9.

Table 4-9 Ksat of soil test results and model results

Soil sample	Test result mm/h	Soil water characteristics model result mm/h
1	28.8	32.93
2	36	32.22
3	7.2	29.36
4	18	31.33
5	14.4	33.29
6	10.8	26.71

The soil water characteristics model have results between 26 and 33 mm/h, this is because the clay content has a significant influence on Ksat while the clay content is not available. In the model, an assumption is made that all the samples have 10% clay content. The only variable is sand content, so the model did not show reliable results. The Ksat input will mainly use test result. To simplify the model, hydraulic conductivity values are mainly related to Land use map (Table 4-10).

Table 4-10 Ksat of different land cover classes

Land use	Landslides	Forest	Shrub and grass	Farmland	Bare land	river
Ksat (mm/h)	36	18	18	28	10.8	0

It is not able to take undisturbed soil samples, and therefore porosity test could not be conducted. The porosity input will be defined by estimation and average soil porosity. The bulk unit weights values were taken from literature. Air entry value, matric suction, and the slope of the SWRC are all related to

unsaturated soil mechanics, and testing these was out of the scope of this MSc research, as it would take too much time. Therefore, most of these values were taken from literature as well. The value and the source of these parameters are shown in Table 4-11.

Table 4-11 Other parameter values and their sources

Parameter	Value	Source
Porosity	0.3	Estimation based on field observation
Bulk unit weight	17 kN/m <sup>3</sup>	constant
Air entry value	0.06	Literature value (Schaap, 1999)
Matric suction	0.5	Literature value (Kutilek and Nielsen, 1994)
Slope of SWRC	14	Literature value (Kutilek and Nielsen, 1994)

#### 4.3.3. Other input data

Based on Bhat's (2016) work in Kashmir, the annual evapotranspiration (ETP) can be calculated by equation (2).

$$E = 221.5 + 29.0 * T \quad (2)$$

E is evapotranspiration, T is annual average temperature. In Rasuwa, the temperature varies from 8 to 30°C, the annual evapotranspiration is about 772.5mm, average 2.11mm/d. According to the temperature, the dry season have ETP of 1.2mm/d and monsoon season has ETP of 3mm/d.

The vegetation condition is not the focus of this study, root cohesion will just link with land use map. Forest has the root cohesion of tree, shrub, grass, and farmland consider the root cohesion of grass and bare land and water have no root cohesion. The root cohesion value derived from literatures (Zhong et al., 2015, Gai, 2013) are maximal root cohesion that influence the soil within the root depth (Table 4-12).

Table 4-12 Maximal root cohesion of different vegetation condition

Land use	Tree	Grass	Bare
Root cohesion (kPa)	29	5	0

While in the modelling, the failure depth is deeper than the root depth and the root cohesion reduction is ignored. The effective root cohesion is considered in the improved modelling.

In the study area, the maximal elevation is 3900m and did not reach the snowline. The snow related parameters are neglected in the modelling. The model start at 1<sup>st</sup> January that is the dry season, the surface detention will be initially zero. Hydrological condition such as ground water level and soil moisture are not available and will be calibrated in the modelling. The initial inputs are shown in Table 4-13.

Table 4-13 Input initial conditions

Initial condition	Groundwater level	Soil moisture	Surface detention	Snow cover	Snow liquid storage
Value	1 m	0.1	0 m	0 m	0 m

During the modelling, the hydrological initial conditions are found not have significant influence on the results. In reality, the groundwater level and soil moisture will be affected by rainfall and recharge. Several water falls were found in study area show that there are groundwater recharge from the bed rocks. While in the STARWARS+PROBSTAB model, recharge is ignored and the rainfall is the only source of the water. The first 150 days of the year have very few precipitation and the initial groundwater level and the soil moisture will decrease to the minimal values.

## 5. RAINFALL THRESHOLDS DEFINITION USING PHYSICALLY-BASED MODELLING

### 5.1. Introduction

#### 5.1.1. Mechanism of rainfall-induced landslides

Rainfall duration and rainfall intensity are all key factors in triggering landslides, especially in Rasuwa area. Rainfall-induced shallow landslides in this research aim to define the movements of slope material within 2 to 3m depth triggered by precipitation. Hydrological factors are the main mechanism of these kinds of failures. For example, Soil moisture will increase the weight and reduced the shearing strength, groundwater level will affect the pore water pressure.

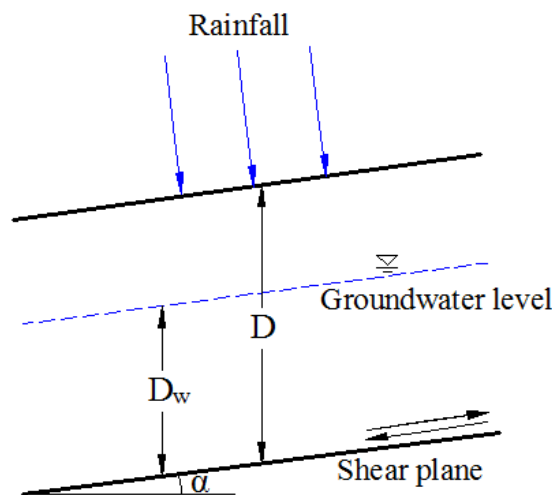


Figure 5-1 Mechanism of rainfall-induced landslides

Rainfall will directly affect the soil moisture and groundwater table, other factors like overflow and discharge are also influenced by rainfall but in the STARWARS model, only soil moisture and groundwater are considered.

#### 5.1.2. Model introduction

STARWARS + PROBSTAB model is developed by van Beek (2002), the original objective is to study the influence of land use and climate change on landslides. The model consists of two separated parts: a dynamic hydrological model STARWARS and an infinite slope stability model PROBSTAB. These two models are closely connected because the outputs of the dynamic hydrological model are the inputs of the slope stability model. The whole model is based on PCRaster and the model script is open source that users can modify the parameters to their own need. According to the landslide characteristics and data availability in Rasuwa, several modifications have been done to adjust this model in the study area.

The STARWARS model is a distributed dynamic hydrological model. The water only comes from rainfall, there is no discharge involve in the model, and the main hydrological process considered in this model is evapotranspiration and infiltration. Evapotranspiration is calculated based on Bhat's work (2016) in Kashmir and be proportional to average temperature. The influence of vegetation on ETP were not taken into consideration. Only vertical infiltration is considered in this mode. Percolation of unsaturated soil will be influenced by the soil water retention curve.

The PROBSTAB model calculates the factor of safety of every pixel column, which is based on failure depth, groundwater level, and soil moisture. This model is based on the infinite slope stability equation of factor of safety:

$$FS = \frac{C_s' + C_r' + \cos^2 \alpha [\gamma(D - D_w) + (\gamma_{sat} - \gamma_w)D_w] \tan \varphi}{\sin \alpha \cos \alpha [\gamma(D - D_w) + \gamma_{sat}D_w]} \quad (3)$$

Where the FS is factor of safety (-),  $C_s'$  is effective cohesion of soil (KPa),  $C_r'$  is effective root cohesion (KPa),  $\varphi$  is internal friction angle ( $^\circ$ ),  $\alpha$  is slope angle ( $^\circ$ ),  $\gamma, \gamma_{sat}, \gamma_w$  are the density of dry soil, saturated soil, and water, D is soil depth,  $D_w$  is groundwater level.

### 5.1.3. Model setup

The input were prepared in Chapter 3 and 4, some input maps are in Appendix 6.

The rainfall input is improved 2015 daily rainfall data, and the time step is set as 1 day. In the original script, the soil was divided into 3 layers and groundwater level is the accumulated height of the whole 3 layers. In this study only first 2 meter soil are considered, and soils are considered only by 1 layer above the slip surface. A is defined as fixed value of 2 meters and if the soil depth is less than 2 meters then the failure depth is defined as soil depth. In the original model, cohesion and root cohesion are fixed values, while cohesion will change under different moisture contents and root cohesion will be affected by soil depth. Cohesion is modified in this work into a dynamic value with equation according to Yang's work (2011) (Figure 4-11).

$$C_s' = -60.1 * \text{theta} + 15.7 \quad (4)$$

Where  $C_s'$  is effective soil cohesion, and theta is soil moisture. This linear ship only tested with soil moisture between 0.006 and 0.24, because the cohesion of soil can never be negative value. If the soil moisture exceed 0.24, the cohesion will be defined as 1.45. The root cohesion will follow the equation (5)

$$C_r' = C_r * (D_r / D_f) \quad (5)$$

Where the  $C_r'$  is effective root cohesion,  $C_r$  is root cohesion,  $D_r$  and  $D_f$  are the depth of root and depth of soil. Root depth of tree and grass are set as 0.5m and 0.1m.

## 5.2. Model results

The precipitation input of 2015 was derived from rainfall station data and GPM data, the rainfall mainly concentrates during monsoon season which is from May 1<sup>st</sup> to September 30<sup>th</sup>. The model output of the year 2015 are shown in Figure 5-2, Figure 5-3, and Figure 5-4. In this rainfall condition a maximum of 6899 pixels become unstable in 2015, which account for 4.5% of the whole study area (153494 pixels). About 50% of the pixels have a minimal FOS value between 0.8 and another 50% between 0.4 and 0.8. Almost no pixel has a FOS lower than 0.4. Half of the unstable pixels have unstable period less than 100 days and several unstable area have more than 150 days of unstable area. These area are mainly old co-seismic landslides that can be easily triggered by rainfall.

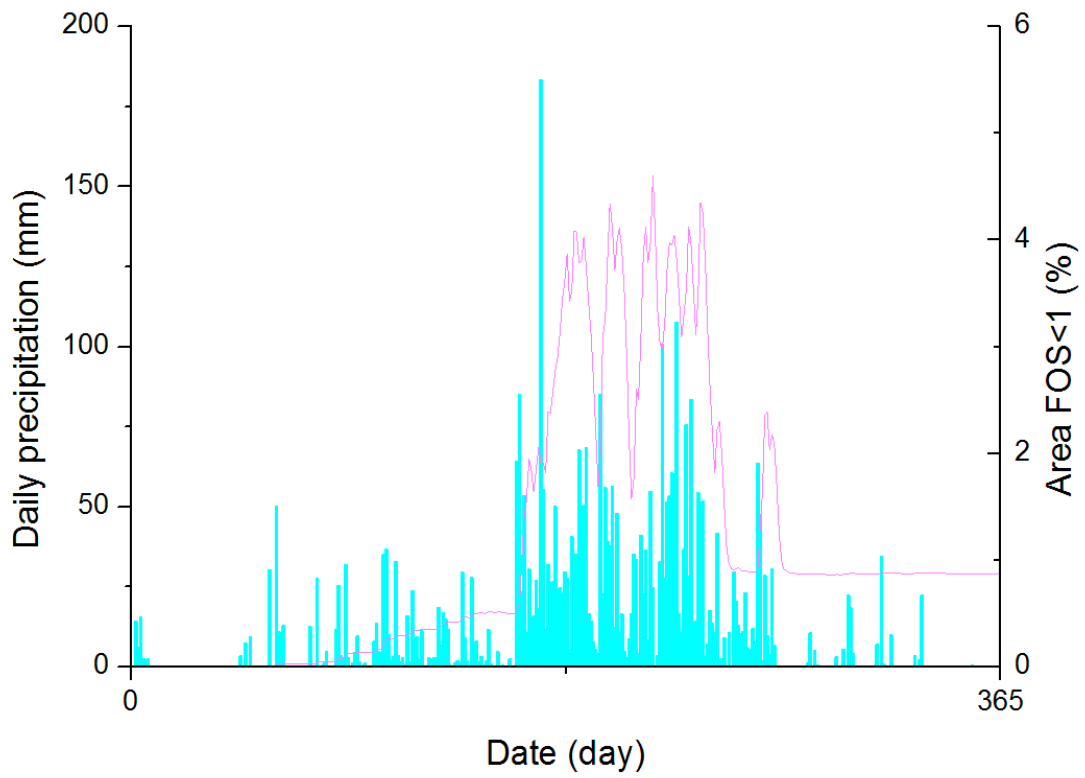


Figure 5-2 Modified 2015 daily rainfall and percentage of FOS<1

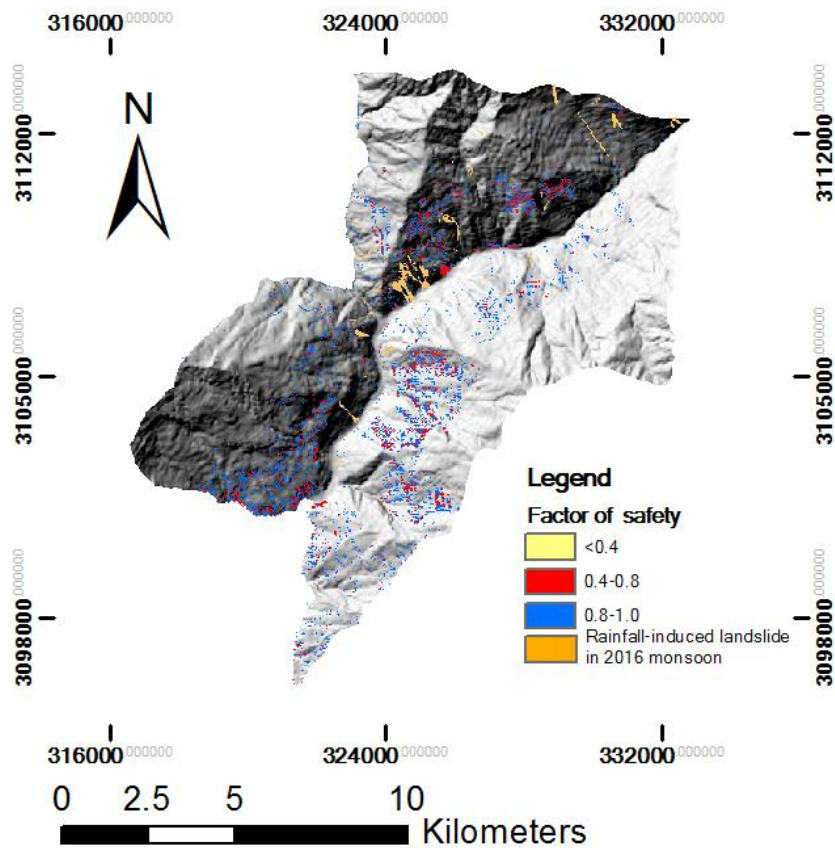


Figure 5-3 Unstable area under 2015 rainfall condition

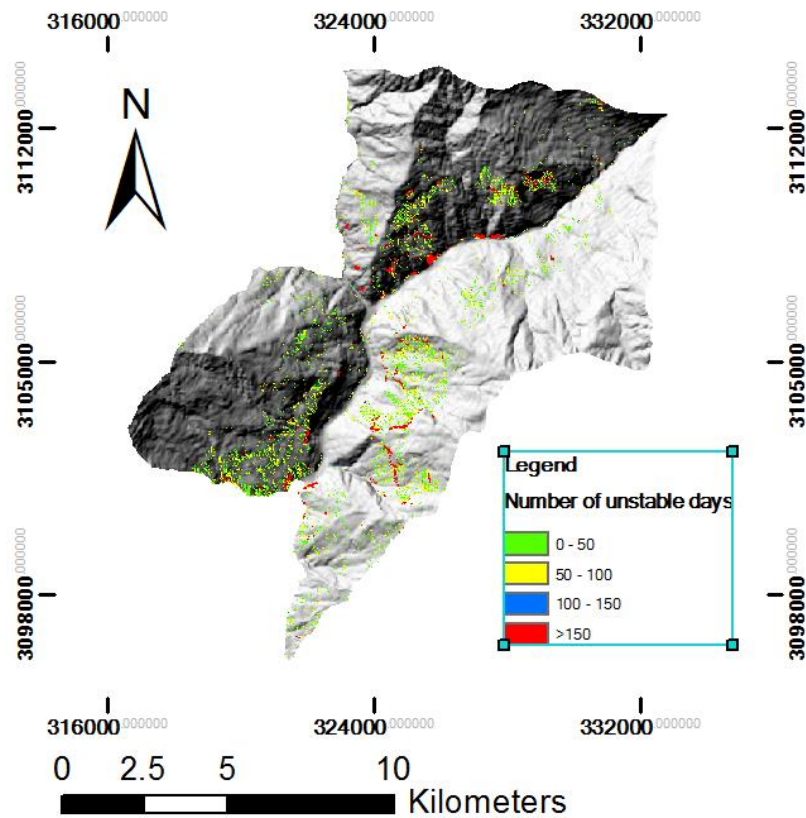


Figure 5-4 Number of unstable days

When comparing the unstable area with the rainfall-induced landslides in 2016, the landslides are not all in unstable areas. But the upper part (source area) of the majority of the rainfall-induced landslides are unstable (Figure 5-5). Because the landslide mapping did not differentiate between source area and runout areas.

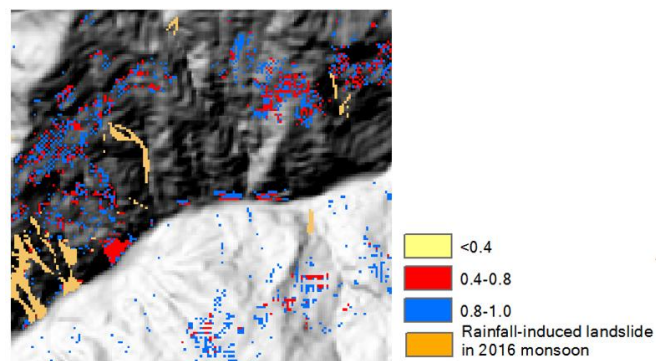


Figure 5-5 rainfall-induced landslides and areas that  $FOS < 1$

In normal model result validation, real landslide data will be used to check the accuracy. In our model, the accurate prediction of specific landslide failure is not possible, due to the large uncertainty of the input factors. In order to do validation without precise landslides information, four specific points with different land use and different slope condition were chosen to validate the model results based on field observation (Figure.5-6, 5-7, 5-8, 5-9). Comparison between the model result and the real condition can be treated as effective validation. The information of the point are shown in Table 5-1.



Table 5-1 Validation points information

	Land use type	Slope steepness	Soil depth	Condition in 2016
1	Barren	49.4	5	New rainfall-induced landslide
2	farmland	29.4	6.8	New rainfall-induced landslide
3	farmland	28.6	4.9	Stable farmland
4	forest	12.8	4.8	Stable forest

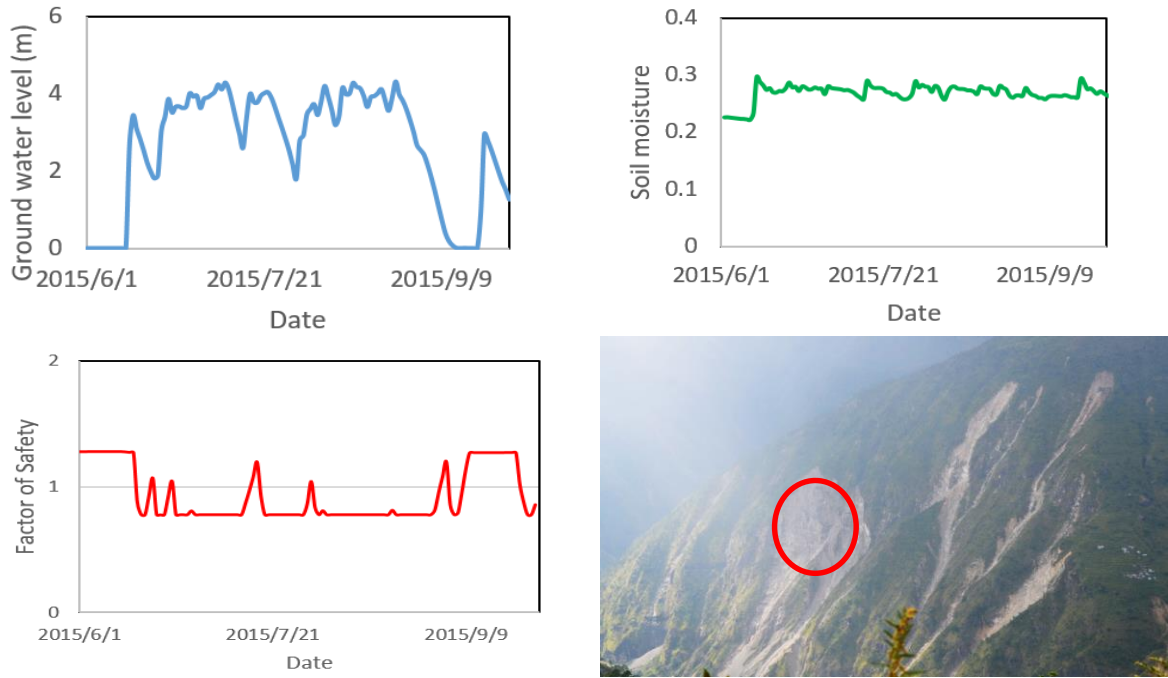


Figure 5-6 a-d The groundwater level, soil moisture, and factor of safe curve during 2015 monsoon of point 1 in unstable bare land

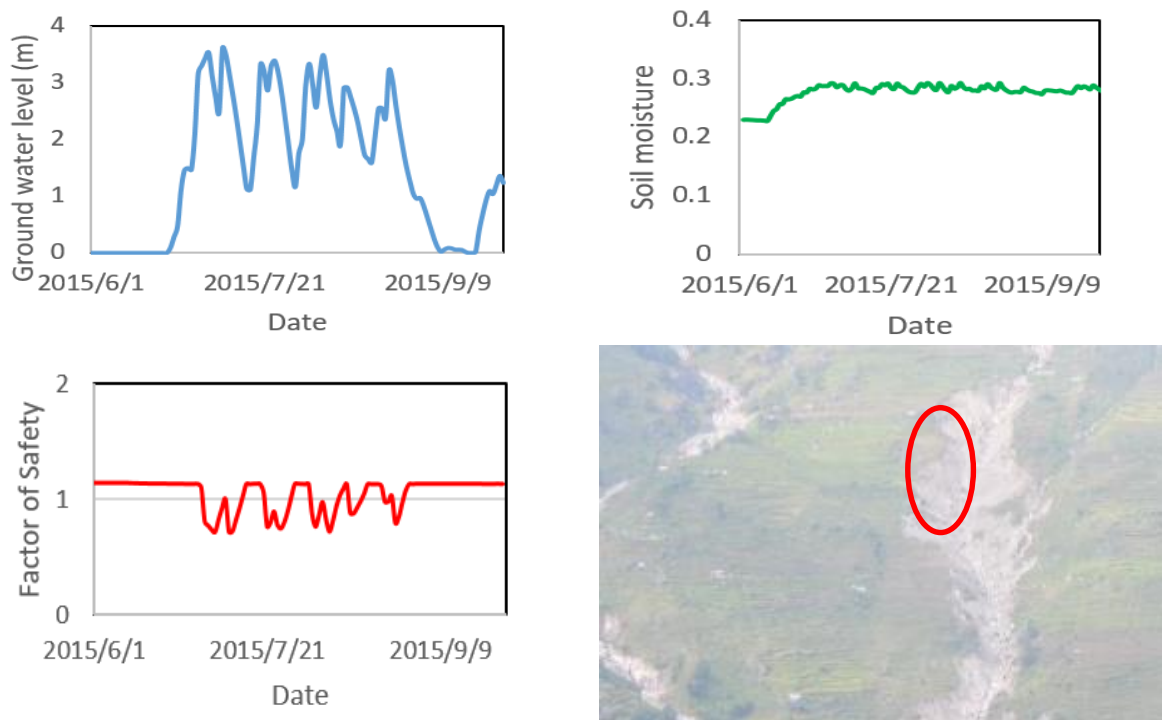


Figure 5-7 a-d The groundwater level, soil moisture, and factor of safe curve during 2015 monsoon of point 2 in unstable farmland

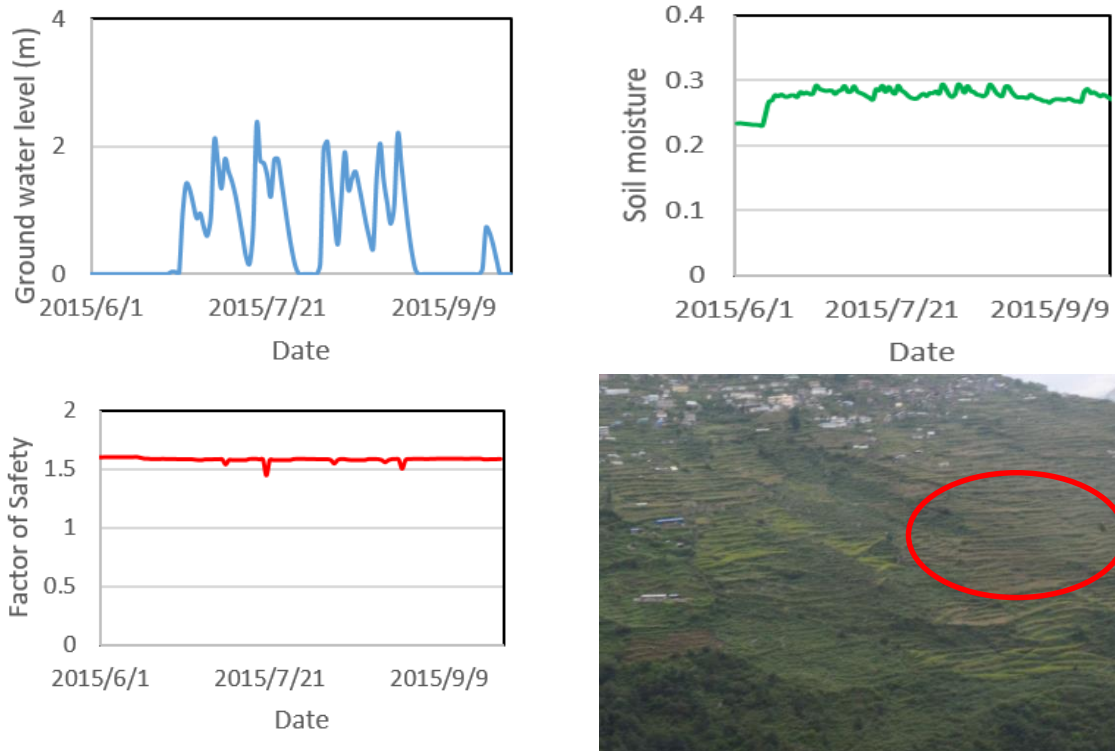


Figure 5-8 a-d The groundwater level, soil moisture, and factor of safe curve during 2015 monsoon of point 3 in stable farmland

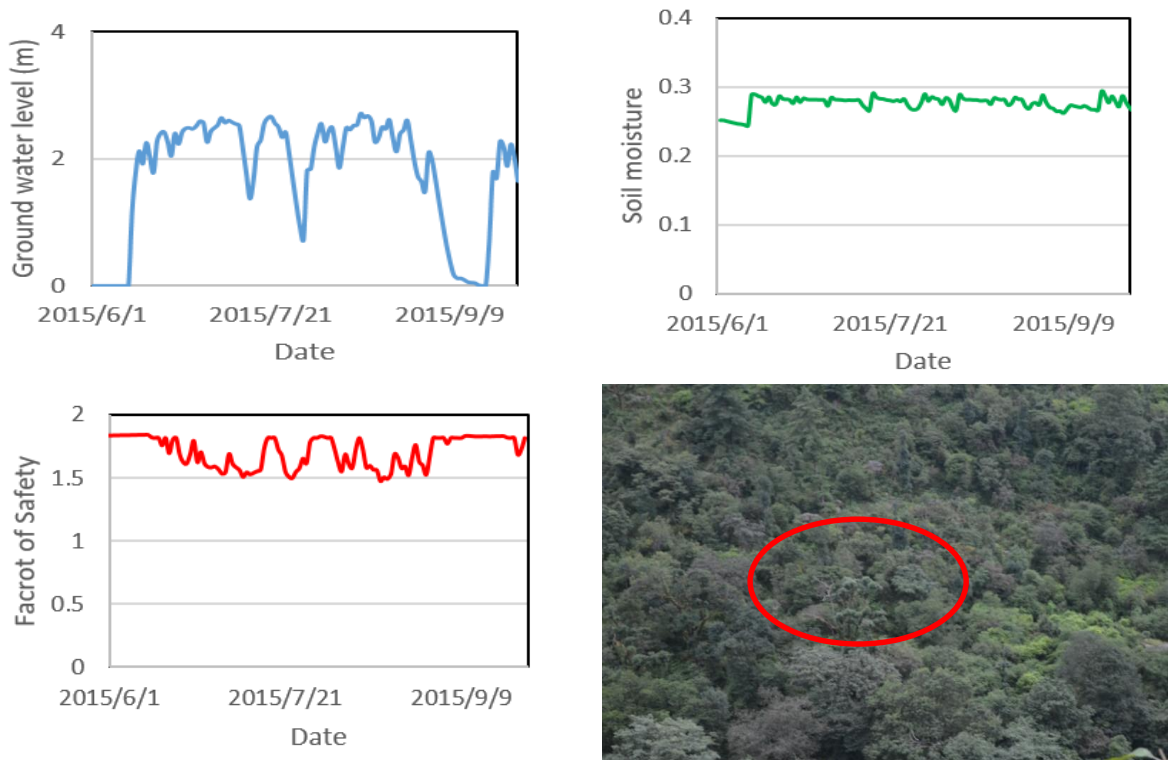


Figure 5-9 a-d The groundwater level, soil moisture, and factor of safe curve during 2015 monsoon of point 3 in stable forest

Conclusion: Point 1 and 2 all have a dynamic safety factor that are often below 1.0 during the monsoon period from May 1<sup>st</sup> to September 30<sup>th</sup>, which indicate that these two areas probably became unstable in 2015 monsoon season. Based on the field investigation, these two areas all have marks of mass movement in 2015. Point 3 and 4 show relative stable FOS during the whole period in the model result. And the reality conditions have the same trends that they are stable area. The analysis in some extent shows the reliability of the STARWARS+PROBSTAB model and the input parameters used in the model.

### 5.3. Intensity-duration rainfall threshold definition

Rainfall threshold are an important component of landslide Early Warning Systems. Mathew et al. (2014) worked in the Garhwal Himalaya India, and got an I-D threshold as (6)

$$I = 58.7 * D^{-1.12} \quad (6)$$

And Dahal & Hasegawa (2008) got an I-D threshold in Nepal Himalaya with equation (7)

$$I = 73.9 * D^{-0.79} \quad (7)$$

In these above thresholds, I is rainfall intensity (mm/h) and D is rainfall duration (h).

All these studies were based on historical landslide inventories and historical rainfall data while none of these data are available in the Rasuwa area. In order to overcome the problem of data absence, physically-based model STARWARS+PROBSTAB were used, as indicated in chapter 1.

Two types of rainfall thresholds were analyzed, using the physically-based modelling approach. Fixed intensity rainfall scenarios were used as input in the intensity-duration threshold definition. The modified 2015 rainfall (Chapter 3) was used in intensity-antecedent rainfall threshold definition.

In empirical intensity-duration threshold definition, historical landslides and matched rainfall datasets are needed. Specific rainfall intensity and duration of actual landslide dates are plotted in the I-D coordinate system. And threshold curves are defined based on the boundaries of the scatters. In order to get the intensity-duration relationship without actual landslide and accurate rainfall data, some modifications are done in the threshold definition. In the physically-based model approach, accurate landslide failure cannot be simulated very well, due to the large uncertainty of the input factors, and the result of the model is the dynamically changing factor of safety for each pixel and slope failure involves more factors rather than simple FOS. The percentage of unstable pixels will replace the actual landslides in the threshold definition.

The average rainfall intensity of 2015 monsoon is 21.23mm/day and the total precipitation is 2591mm. The time step was set as 1 day and end time was set at 50 days. The reason for using 50 days as the end time is to compare the model result between the extreme condition and 2015 rainfall condition that almost have the same amount of accumulated precipitation. Fixed rainfall scenarios were used in the model in order to simplify the rainfall pattern. The rainfall input from 10 mm/day to 50 mm/day were defined as input in the model and the results are shown in Figure.5-10.

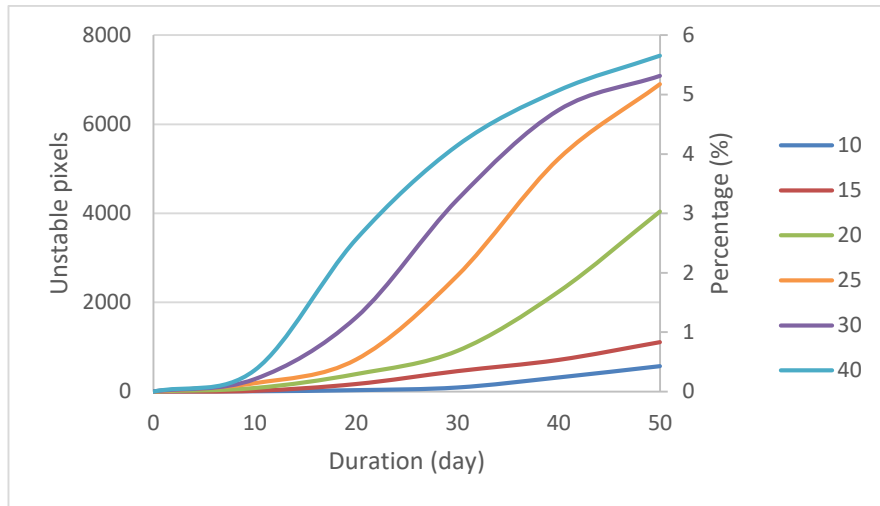


Figure 5-10 The result of model. Numbers of unstable pixels ( $FOS < 1$ ) change

Figure 5-10 shows that the unstable pixel number reaches almost 8000, 5.2% of the whole study area, under the most extreme rainfall condition of 50mm/day lasting 50 days. This result is higher than the model result of 2015 rainfall condition (6899 pixels). Consider single rainfall events, this kind of rainfall is nearly impossible in reality. While from the over view of 2015 precipitation of monsoon, long-term rainfall with average rainfall intensity of 50mm/day is possible. These results show the different rainfall response patterns. In 2016 monsoon season, rainfall induced landslide take about 1081 pixels (0.67%) in study area. This statistic is based on field landslide mapping. This number takes 12.5% of the potential unstable area and 0.67% of the whole study area. This number is set as the baseline of rainfall thresholds.

In threshold definition, based on 2016 rainfall induced landslides areas. 1000 pixels (0.67% of whole potential unstable area), 2000 pixels (1.33%), and 4000 pixels (2.67%) are set as boundary of rainfall thresholds. 10mm/day rainfall did not reach the baseline of 1000 pixels so it was ignored in threshold definition.

The scatters of rainfall duration and rainfall intensity are plot in logarithmic coordinate system. Linear correlation were very clear between these two variables.

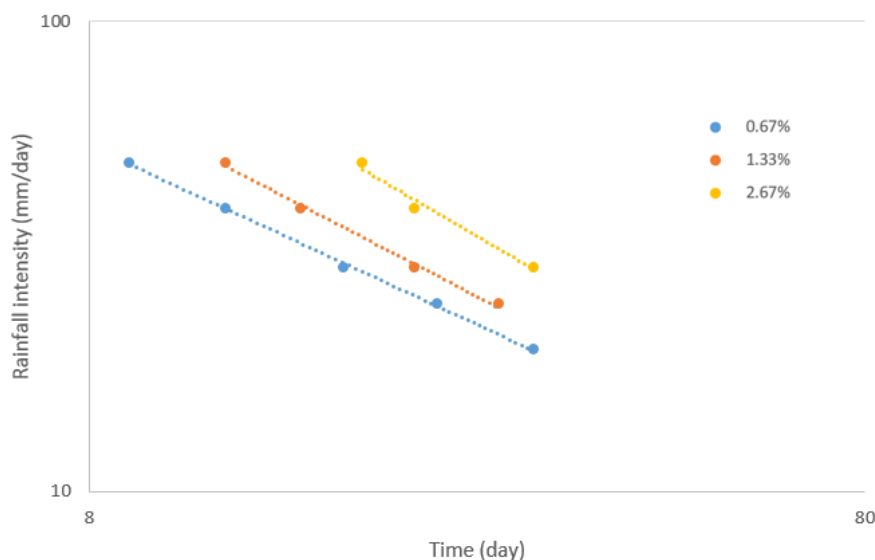


Figure 5-11 The I-D rainfall thresholds

The thresholds can be presented with the follow equations:

$$I = 263.24 * D^{-0.759} \quad (8)$$

$$I = 410.13 * D^{-0.854} \quad (9)$$

$$I = 791.42 * D^{-0.966} \quad (10)$$

The I in the equation is daily rainfall (mm/day) and duration unit is day. If transfered into mm/h, the equations will be presented as:

$$I = 122.38 * D^{-0.734} \quad (11)$$

$$I = 257.55 * D^{-0.788} \quad (12)$$

$$I = 710.55 * D^{-0.861} \quad (13)$$

Where I is rainfall intensity (mm/hour) and D is duration (hour). Compared with the result of Mathew and Dehal, these thresholds show similar patterns (Figure 5-12). While under same duration, landslides can be triggered under lower rainfall intensity, which means the product from STARWARS+PROBSTAB has underestimation about rainfall-induced landslides.

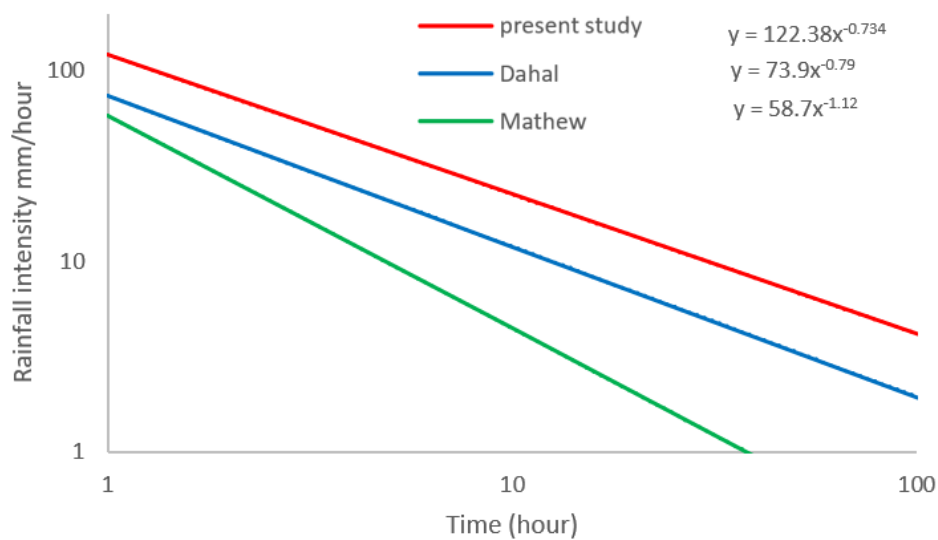


Figure 5-12 Threshold of Dahal (2008), Mathew (2014), and present study

One of the possible reason for the underestimation is the baseline used in threshold definition. The baseline was set based on 2016 rainfall induced landslides, and the landslides mapping also include the deposit area that enlarge the landslide area. Another problem is the missing of validation and cabrination. More detailed actual landslide data are needed to improve the rainfall thresholds.

#### 5.4. Intensity-antecedent rainfall threshold definition

Intensity-Duration is not the only way of rainfall threshold definition. An extensive overview of rainfall threshold methods, and its applications for different regions is provided by <http://rainfallthresholds.irpi.cnr.it/>. The first limitation of I-D thresholds is that duration just take rainfall days into account and does not consider the rainfall difference between days nor the antecedent rainfall.

Antecedent rainfall may play an important role in the triggering of deep landslides, and often also has significant effects for shallow landslides. The soil moisture and groundwater as after the rainfall stops will have a delayed effect because of the soil hydrological characteristics. This kind of delay means the antecedent rainfall will influence the factor of safety of the current situation.

Thresholds have been established with intensity and antecedent rainfall in many areas. For example Tien Bui et al., (2013) applied daily-antecedent rainfall threshold in Vietnam, and 3-day to 30-day antecedent rainfall are considered. Different duration leads to different threshold pattern. 15-day antecedent rainfall was chosen and the threshold is as equation (14)

$$R_{TH} = 128.5 - 0.164R_{15}. \quad (14)$$

Gabet et al (2004) developed rainfall threshold for sediment peaks in Nepal, the threshold is presented as Figure 5-13.

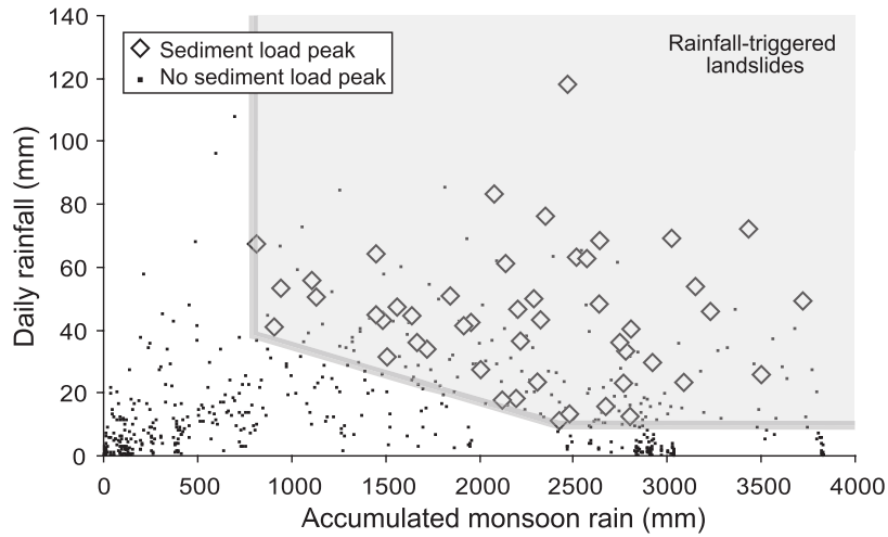


Figure 5-13 I-A rainfall threshold defined by Gabet et al (2004)

Dahal & Hasegawa (2008) considered daily rainfall and accumulated monsoon rainfall in Nepal and got a threshold which could not be defined clearly by an equation due to large scatter of data. Their work not only considered shallow landslides, but also deep-seated landslides.

In order take the antecedent rainfall into consideration, the rainfall obtained for the monsoon of 2015 (as described in Chapter 3) was used in the STARWARS+PROBSTAB model. The antecedent rainfall was calculated based on equation (15) (Glade et al., 2000)

$$R_{ant} = kR_1 + k^2R_2 + k^3R_3 + \dots + k^nR_n \quad (15)$$

In which  $R_{ant}$  is antecedent rainfall,  $R_n$  is the daily rainfall of the nth day before the current day and  $k$  is a constant related to outflow. In several publications the  $k$  is set as 0.84, which come from the study in US (Bruce & Clark, 1966, Crozier, 1980). This value is related to streamflow data which is not available for Rasuwa area. Improvement can be done with more data.

In order to determine the best intensity-antecedent rainfall threshold, several options of antecedent rainfall were calculated: 5-day, 10-day, and 30-day (Figure 5-14)

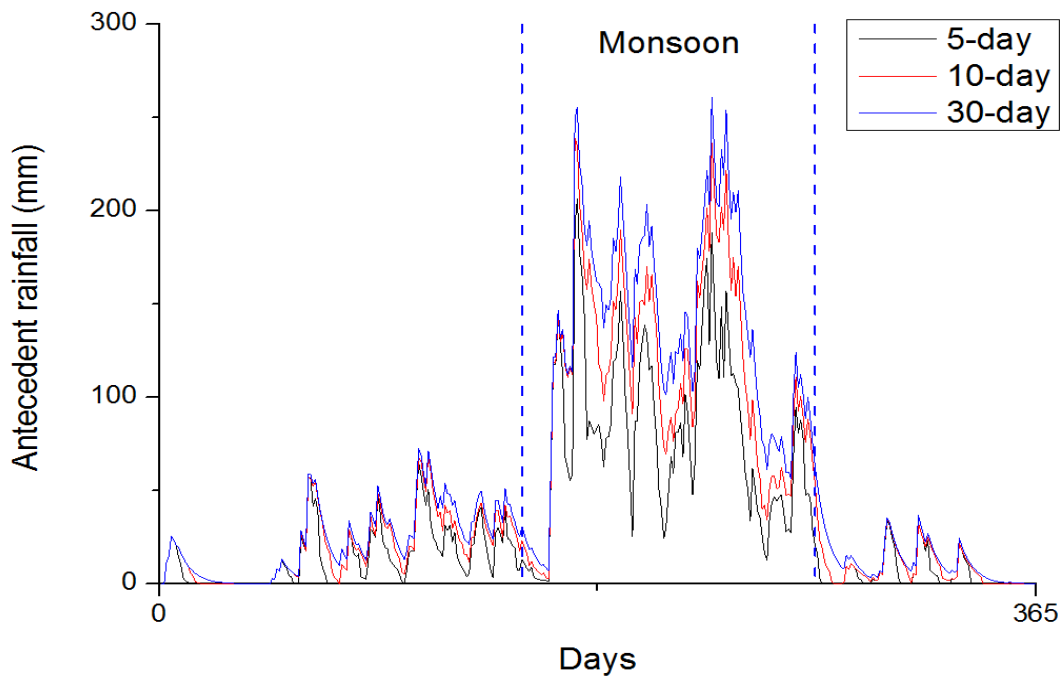
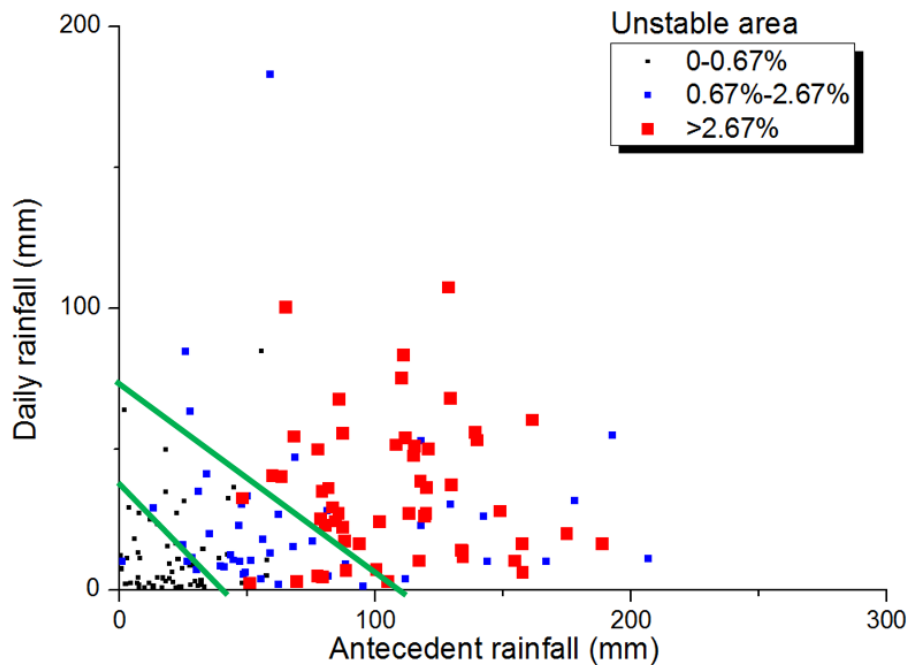


Figure 5-14 Different antecedent rainfall curves.

The graph reveals that the longer the duration, the less variation in antecedent rainfall. The curve is relatively smooth. This smoothing effect reduces the influence of the errors in rainfall data, although when using them in combination with daily data these are still very important.

The output of the 2015 simulation in chapter 5.2 were used. New script was add in the model to derive the unstable pixel numbers from the FOS time series maps. The scatters of daily rainfall and antecedent rainfall are plotted. The boundary was follow the I-D thresholds 0.67% and 2.67%.



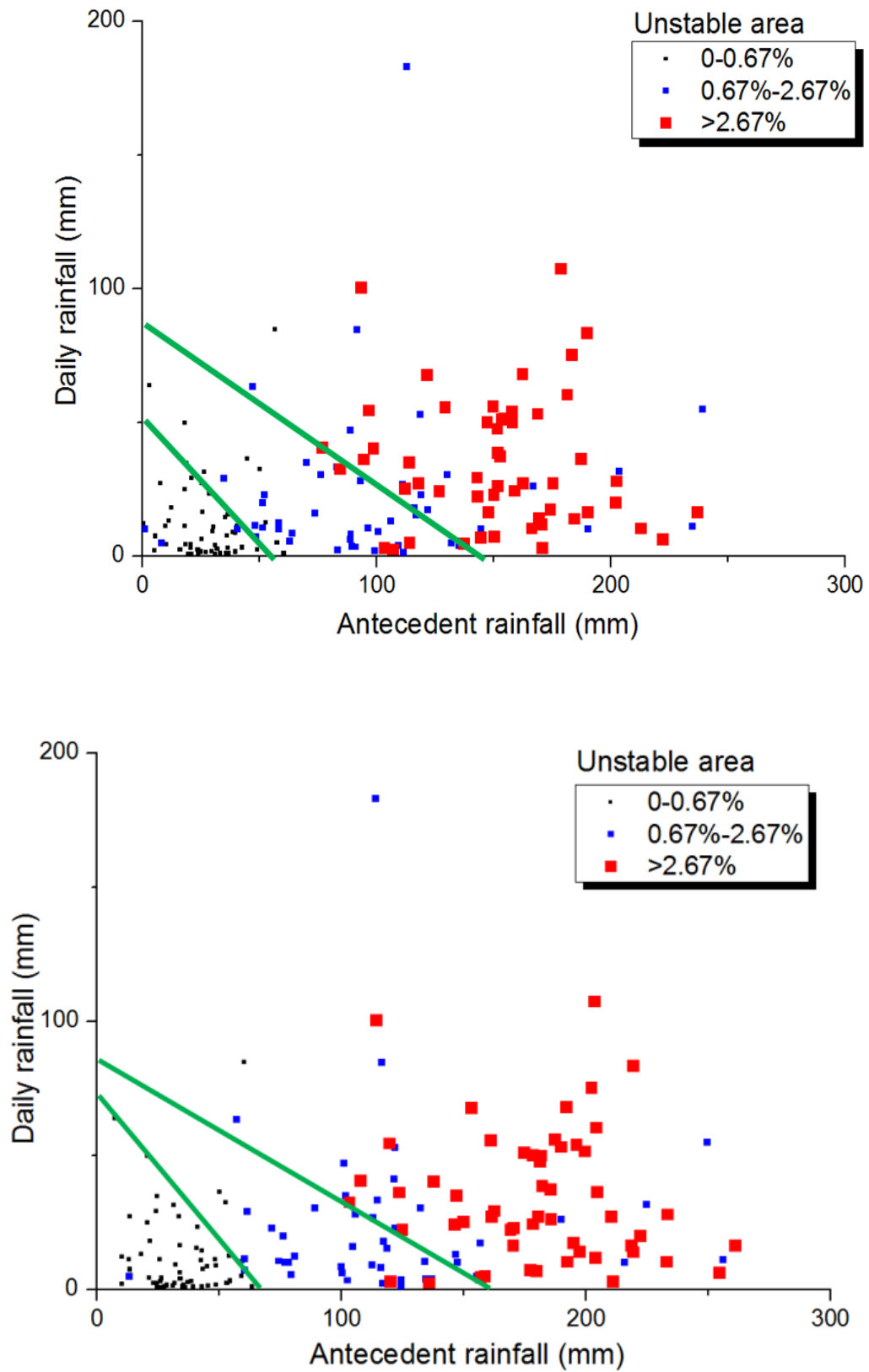


Figure 5-15 a, b, c The scatter graph of 5-day, 10-day, 30-days antecedent versus daily rainfall. The points show the percentage of unstable pixels during the year 2015.



The days in 2015 that caused instability in 0.67% part of the study area and distributed in the lower left corner of the graph, with small antecedent and daily rainfall values. In the 5-days and 10-days graphs the boundary of 0.2% have some mixed points and in the 30-day graph, the boundary is quite clear. All 3 graphs do not have a very clear boundary for the 2.67% unstable area. The pattern of days above 2.67% is relatively regular but those of 0.67% to 2.67% have a dispersive distribution. When comparing the 3 graphs, the 30-day antecedent rainfall seems to have the best performance, although there are no objective methods applied to substantiate this. The distribution of the 3 group of scatters was used as the basis of threshold definition. Based the scatter distribution, threshold lines were manually defined based on 30-day antecedent rainfall.

The threshold equations could the be defined as follows:

$$I = 70 - R_{ant} \quad (16)$$

$$I = 90 - 0.56R_{ant} \quad (17)$$

I is average daily rainfall,  $R_{ant}$  is the antecedent rainfall. Compare with Tien Bui's(2013) result equation (11), the result is similar.

According to the local people, one landslide occurred at the first two weeks of 2016 monsoon (Figure 5-16). This rainfall-induced shallow landslides have a continuous failure for several days.



*Figure 5-16 The landslides triggered by first two weeks of 2016 monsoon*

14 daily rainfall and antecedent rainfall data start from the beginning of the 2016 monsoon are plotted in the scatters (Figure 5-17).

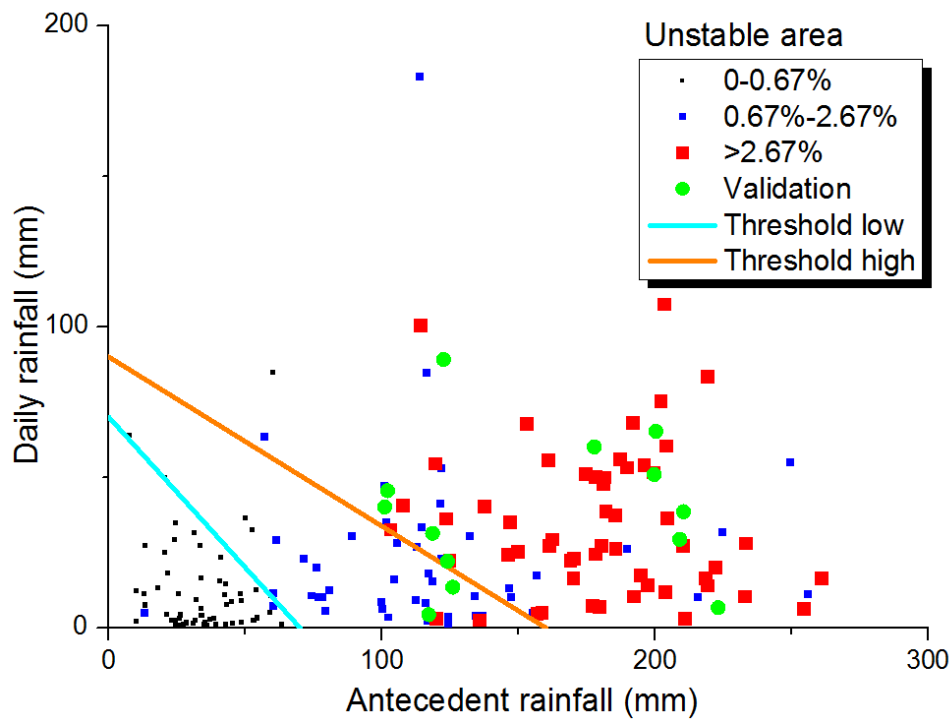


Figure 5-17 Validation using first two week rainfall data from 2016 monsoon

The scatters of these 14 days mainly located in area over threshold high, 2 points are located in moderate area. According to the threshold, during the first two weeks of 2016 monsoon many area might become unstable. But for single specific landslide cannot be simulated by this threshold. So more landslide data are need for validation.

### 5.5. Summary

The simulation of 2015 rainfall scenario was done based on STARWARS+PROBSTAB modelling. According to the model results, 4.5% of the study area become unstable and more than half of these area have the unstable statement over 50 days. While in reality, the 2016 rainfall-induced landslides only cover 0.67% of the study area which is far less than 4.5%. This trend indicate the overestimation of the modelling which will lead to many False Positives, and no False Negatives. Therefore the practical application of using this as a basis for Early Warning Systems is very limited. Much more work is needed to properly parameterize the model and calibrate it.

We attempted to define two types of rainfall thresholds based on STARWARS+PROBSTAB physically-based modelling. All the thresholds show rather clear boundaries of different landslide conditions. However, all these thresholds is based on physically-based modelling which produced the theoretical value of factor of safety. These FOS cannot refer to real instability because the shallow landslide failure involves more factors. And the rainfall thresholds are not fixed value that they may have changed after major events such as earthquakes, this phenomenon is also shown in China after Chi-Chi earthquake Wenchuan earthquake (Lin et al., 2006; Tang et al., 2009).

## 6. DISCUSSION, CONCLUSION, AND SUGGESTION

### 6.1. Discussion

The research was hindered by the lack of appropriate data: rainfall records, historical landslide occurrences, soil data and digital elevation data were all not optimal for this remote study area in Nepal.

The ideal rainfall input should be calibrated GPM data. But the rainfall station data and GPM data do not have a good linear correlation. Rainfall spatial distribution in mountain area is a complex problem that involves many topographic factors especially in high elevation area like Himalaya. And rainfall station data in this research were only available till 2015, whereas GPM data started to become available from April 2015. The quantity of data may be not enough for satellite data calibration.

The study area in Rasuwa turned out to be less suitable for this type of modelling than expected before going in the field. Many of the events in the study area were caused by the 2015 Gorkha earthquake under specific conditions of topographic amplification. Most of the co-seismic landslide phenomena were not shallow landslides, but rockfalls, debris-avalanches, and relatively deep failure in weathered rocks. Therefore the modelling of shallow failures using a physically-based model that assumes homogenous soil characteristics and instability in the upper meter was not considered very realistic. Many of the soils were also coarse grained, and related to colluvial origin.

Parameterization of the physically-based model was a difficult task in this study due to the lack of reliable information. Detailed soil parameter maps were not available in this area. Filling all the missing data by field investigation was not possible in limited time. Besides the parameters from laboratory tests, all other parameters were derived from literature or defined by estimation and field observation. These assumptions increased the uncertainty of the modelling. The study will be providing more realistic results if better soil and rock mechanical characteristics could be obtained and other landslide-related information.

The STARWARS+PROBSTAB model originally was designed to study the influence of land use and climate change on landslides. Vegetation plays a very important role in this model. Because vegetation is not the focus in this study, the majority of the vegetation-related parameters are simplified into single values through the whole area. Further study can be done to analyze the vegetation influence in Rasuwa area because the ecological methods are cost-effective ways of landslide hazard reduction. There is a problem of groundwater level, underground recharge is ignored in the model and infiltration must be higher than reality to maintain the groundwater level in a reasonable level. A relative groundwater table may be helpful in the water stimulation which can be used to do the validation for the hydrological model. The PROBSTAB model using infinite slope model equations and using fixed cohesion. Actually, cohesion is significantly influenced by soil moisture. In this study, the cohesion is linked with soil moisture with the relation derived from literature. The relation varies a lot from different soil type and clay content. This modification can increase the FOS sensitivity with rainfall.

About 8000 pixels that 5.3% of the whole study area become unstable under the 2015 rainfall scenario. While in 2016 monsoon, the rainfall induced landslides only take area of 0.67% in study area. The model result has the problem of overprediction that will lead to many False Positives, and no False Negatives. Therefore the practical application of using this as a basis for Early Warning Systems is very limited. Much more work is needed to properly parameterize the model and calibrate it.

Two types of rainfall thresholds were defined based on the physically-based modelling. Several small points are used to validate the model, but no validation had been done to test the thresholds. Because no accurate landslide dates that matched with the triggering rainfall were available. Rainfall-induced shallow landslides are distinguished during the field work and several visits had been paid to local communities, soil and water department, offices and schools in Dhunche (main city in Rasuwa area). No accurate record had

been made. Regional landslide mapping and accurate triggering time should be acquired to validate the performance of rainfall thresholds. Enlarge the rainfall dataset is also helpful to the thresholds.

The thresholds are not constant values that they may have changed after major events such as earthquakes. This kind of change is mainly because of the events destroy the soil and rock structure and leave fractures on the slope surface. The fractures increase the infiltration speed and static water pressure. It is difficult to take this factor into consideration for physically-based model like STARWARS+PROBSTAB model. Which means the model result will not significantly change after extreme events as in reality.

The result of modelling only represent the theoretical instability using factor of safety, there are two measures to improve the result to relate this value to realistic instability. Qualified real data can be used in the modelling to improve the model result. Validation and calibration can be done to improve the thresholds.

The thresholds are the initial part of EWS, detailed warning such as using the results to derive frequency of landslides in order to determine hazard (probability of occurrence) and risk is difficult. The uncertainty of the geotechnical parameters should be taken into account. Which need large-scale detailed field work that will cost lot of money and source. So the current product can be used in general warning and prediction linked with weather forecast.

## 6.2. Conclusion

Rainfall thresholds as a component of a regional Landslide Early Warning System using satellite-derived rainfall in combination with physically-based landslide initiation modelling have been developed under the condition with very limited data.

Multiple rainfall data analysis was carried out mainly based on Pearson correlation coefficient and significance calculation. Tropical Rainfall Measuring Mission satellite (TRMM) data have the worst performance in the study area. The data has very low resolution, low significance with respect to the other data sources, and abnormal values during the monsoon season. Rainfall station data should be the most reliable and accurate data on precipitation as it records the actual daily amounts in different locations within the study area. However, the exact locations of the stations are a source of uncertainty, and the records gives rise to doubts, as the manual recording increases the uncertainty of the data. Large number of missing data is another problem. Global Precipitation Measurement (GPM) data have a better performance in this area, high spatial and temporal resolution, no data gaps, and significant correlation with the rainfall station data. The problem of Global Precipitation Measurement (GPM) data is the lacking of calibration. The algorithm of the GPM data is mainly based on the cloud temperature and cloud depth while the rainfall spatial distribution in mountain area involves more topography factors especially in high mountain areas like Himalaya. The best solution for obtaining rainfall data sets was to use GPM data calibrated by rainfall station data. The calibration work cannot be finished because of the quality of rainfall station data and the available period of GPM data start from April 2015. The maximal value of the rainfall station data and GPM data was used as input of the physically-based model. The maximum values ensure the extreme rainfall events will not be missed, but there is a large chance that the total rainfall will be higher than reality. Accurate slope failure time and location cannot be simulated by the model, the percentage of the unstable areas were used instead, so the higher rainfall will not be a severe problem.

Soil depth modelling is crucial for this type of physically-based modelling. However, it is also one of the largest unknown factors. It is not possible to make a soil depth map based on field observation. And the modelling will lead to very large generalisations. The soil depth is stimulated by using the soil depth model developed by Kuriakose et al., (2009). The soil depth model is mainly based on elevation and distance to streams. The soil condition in Rasuwa is complex, and human activities and historical landslides have important influence on soil depth. Small modifications were done to add extra depth related to land use

and land cover and the result shows a better correlation with field investigation. The only available soil parameters come from the laboratory test. The parameterization with limited information is mainly relied on literature data as there was no possibility to carry out sufficient field and laboratory testing.

The main mechanism of rainfall-induced landslide is the rainfall saturated the soil layer reduced the shear strength. The resistant force decrease till less than driving force and the slope become unstable. In this process, rainfall, soil, and topography all play important roles. In the STARWARS+PROBSTAB model, several assumptions were made to simplify the simulation. The modelling setup was changed to only 1 layer above the slip surface. STARWARS divide each soil layer into a saturated zone and unsaturated zone, and the water level is calculated based on water level from last time step and soil moisture change. The only source of water is rainfall and only vertical fluxes are considered, underground recharge, and river recharge are ignored. Buoyancy is the only water pressure considered in the infinite slope model, while in reality static and dynamic water pressure also play important roles in slope stability. And cohesion has a linear relationship with soil moisture.

The model output could not be validated with historical landslide dates and locations, as these were not available. Therefore the results were checked by analyzing the results from four specific points. The model results of 2015 show the same trend as real conditions based on filed observations. The factor of safety shows clear correlation with rainfall.

Two types of rainfall thresholds were defined based on the physically-based modelling. Intensity-duration threshold can be presented as:

$$I = 263.24 * D^{-0.759} \quad (8)$$

$$I = 410.13 * D^{-0.854} \quad (9)$$

$$I = 791.42 * D^{-0.966} \quad (10)$$

The I in the equation is daily rainfall (mm/day) and duration unit is in days.

The intensity-antecedent rainfall threshold equations are presented as follows:

$$I = 70 - R_{ant30} \quad (16)$$

$$I = 90 - 0.56R_{ant30} \quad (17)$$

I is daily rainfall intensity,  $R_{ant30}$  is the 30-day antecedent rainfall.

### 6.3. Suggestion

- (1) GPM satellite rainfall data calibration in mountain area is an interesting challenge for future research.
- (2) Further study can be done to analysis the vegetation influence in Rasuwa area because the ecological methods are cost-effective ways of landslide hazard reduction.
- (3) Validation and calibration work are needed to relate the theoretical thresholds with actual landslide instability.
- (4) More emphasis should be given to keep records of the location and dates of landslide events, and a national landslide database should be established.
- (5) The threshold is only one part of the EWS, the monitoring, alert, and social response are need to establish an integrated EWS.
- (6) The short-term rainfall threshold focus on extreme rainfall events within 24 hour could be done based on improved OpenLISEM model.

## LIST OF REFERENCES

- Barros, A. P., Joshi, M., Putkonen, J., & Burbank, D. W. (2000). A study of 1999 monsoon rainfall in a mountainous region in central Nepal using TRMM products and rain gauge observations. *Geophysical Research Letters*, 27(22), 3683–3686. <https://doi.org/10.1029/2000GL011827>
- Baum, R. L., & Godt, J. W. (2010). Early warning of rainfall-induced shallow landslides and debris flows in the USA. *Landslides*, 7(3), 259–272. <https://doi.org/10.1007/s10346-009-0177-0>
- Baum, R. L., Savage, W. Z., & Godt, J. W. (2002). TRIGRS — A Fortran Program for Transient Rainfall Infiltration and Grid-Based Regional Slope-Stability Analysis, Version 2.0. *U.S. Geological Survey Open-File Report*, (2008–1159), 75. <https://doi.org/Open-File Report 2008–1159>
- Bhat, S. A., Meraj, G., & Pandit, A. K. (2016). Assessing the influence of stream flow and precipitation regimes on water quality of the major inflow stream of Wular Lake in Kashmir Himalaya, 1–15. <https://doi.org/10.1007/s12517-015-2083-1>
- Bookhagen, B., & Burbank, D. W. (2006). Topography, relief, and TRMM-derived rainfall variations along the Himalaya. *Geophysical Research Letters*, 33(8), 1–5. <https://doi.org/10.1029/2006GL026037>
- Bruce, J. P., & Clark, R. H. (1966). *Introduction to Hydrometeorology* Pergamon Press. Long Island City, NY.
- Burroughs, W. (1999). *The Climate Revealed*. Cambridge University Press.
- Capparelli, G., & Tiranti, D. (2010). Application of the MoniFLaIR early warning system for rainfall-induced landslides in Piedmont region (Italy). *Landslides*, 7(4), 401–410. <https://doi.org/10.1007/s10346-009-0189-9>
- Capparelli, G., & Versace, P. (2011). FLAIIR and SUSHI: Two mathematical models for early warning of landslides induced by rainfall. *Landslides*, 8(1), 67–79. <https://doi.org/10.1007/s10346-010-0228-6>
- Collins, B. D., & Jibson, R. W. (2015). Assessment of Existing and Potential Landslide Hazards Resulting from the April 25, 2015 Gorkha, Nepal Earthquake Sequence. *U.S. Geological Survey Open-File Report*, (August), 50. <https://doi.org/10.3133/ofr20151142>
- Crozier, M. J., & Eyles, R. J. (1980). Assessing the probability of rapid mass movement. In *Third Australia-New Zealand conference on Geomechanics: Wellington, May 12-16, 1980* (p. 2). Institution of Professional Engineers New Zealand.
- Dahal, R. K., & Hasegawa, S. (2008). Representative rainfall thresholds for landslides in the Nepal Himalaya. *Geomorphology*, 100(3–4), 429–443. <https://doi.org/10.1016/j.geomorph.2008.01.014>
- Devi, S. R. (2014). Daily Rainfall Forecasting using Artificial Neural Networks for Early Warning of Landslides, (November 1993), 2218–2224.
- Dhakal, S. (2016). Disasters in Nepal. *Disaster Risk Management*, (July 2015), 39–74.
- Dietrich, W. E., Asua, R. R. de, Orr, J. C. B., & Trso, M. (1998). A validation study of the shallow slope stability model, SHALSTAB, in forested lands of Northern California by Department of Geology and Geophysics University of California Berkeley, CA 94720 and Rafael Real de Asua Martin Trso Stillwater Ecosystem, W. *Landslides*, (June 1998), 59.
- DPNet. (2013). *Nepal Disaster Report, Disaster Preparedness Network, Nepal*.
- Fallis, A. . (2013). *Landslide Analysis and Early Warning Systems. Journal of Chemical Information and Modeling* (Vol. 53). <https://doi.org/10.1017/CBO9781107415324.004>
- Gabet, E. J., Burbank, D. W., Putkonen, J. K., Pratt-sitaula, B. A., & Ojha, T. (2004). Rainfall thresholds for landsliding in the Himalayas of Nepal, 63, 131–143. <https://doi.org/10.1016/j.geomorph.2004.03.011>
- Gai, X. (2013). *Study of Mechanical Properties of Tree Root Reinforcing Soil*. Beijing Forestry University.
- Galanti, Y., Giannecchini, R., Avanzi, G., Barsanti, M., & Benvenuto, G. (2016). Rainfall thresholds for triggering shallow landslides in Vara Valley (Liguria, Italy). *Landslides and Engineered Slopes. Experience*,

- Theory and Practice*, (July), 943–950. <https://doi.org/10.1201/b21520-111>
- Gaona, M. R., Overeem, A., Leijnse, H., & Uijlenhoet, R. (2016). First-Year Evaluation of GPM Rainfall over the Netherlands: IMERG Day 1 Final Run (V03D). *Journal of Hydrometeorology*, 17(11), 2799–2814.
- Gautam, D. K., & Phajju, A. G. (2013). Community Based Approach to Flood Early Warning in West Rapti River Basin of Nepal. *IDRiM*, 3(1). <https://doi.org/10.5595/idrim.2013.0060>
- Glade, T., Crozier, M., & Smith, P. (2000). Applying Probability Determination to Refine Landslide-triggering Rainfall Thresholds Using an Empirical “ Antecedent Daily Rainfall Model ,” 157, 1059–1079.
- Green, W. H., & Ampt, G. A. (1911). Studies on Soil Physics. *The Journal of Agricultural Science*, 4(01), 1–24.
- Guzzetti, F., Peruccacci, S., Rossi, M., & Stark, C. P. (2008). The rainfall intensity-duration control of shallow landslides and debris flows: An update. *Landslides*, 5(1), 3–17. <https://doi.org/10.1007/s10346-007-0112-1>
- HRRP. (2016). Rasuwa district - Landslide susceptibility. Retrieved from <http://hrrpnepal.org/maps/map-and-infographics/thematic-maps/rasuwa-district-landslide-susceptibility/>
- Jetten, V. G., & de Roo, A. P. (2001). Spatial analysis of erosion conservation measures with LISEM. In *Landscape erosion and evolution modeling* (pp. 429–445). Springer US.
- Karki, R. (2000). Status of Automatic Weather Stations in Nepal and Comparison of Air Temperature and Precipitation Data Between Automatic Weather Station and Manual Observation. Retrieved from [https://www.wmo.int/pages/prog/www/IMOP/publications/IOM-104\\_TECO-2010/P3\\_8\\_Karki\\_Nepal.pdf](https://www.wmo.int/pages/prog/www/IMOP/publications/IOM-104_TECO-2010/P3_8_Karki_Nepal.pdf)
- Kirschbaum, D. B., Stanley, T., & Simmons, J. (2015). A dynamic landslide hazard assessment system for Central America and Hispaniola. *Natural Hazards and Earth System Science*, 15(10), 2257–2272. <https://doi.org/10.5194/nhess-15-2257-2015>
- Kirschbaum, D., Stanley, T., & Yatheendradas, S. (2016). Modeling landslide susceptibility over large regions with fuzzy overlay. *Landslides*, 13(3), 485–496. <https://doi.org/10.1007/s10346-015-0577-2>
- Kuriakose, S. L., Devkota, S., Rossiter, D. G., & Jetten, V. G. (2009). Prediction of soil depth using environmental variables in an anthropogenic landscape, a case study in the Western Ghats of Kerala, India. *Catena*, 79(1), 27–38. <https://doi.org/10.1016/j.catena.2009.05.005>
- Kutilek, M., & Nielsen, D. R. (1994). *Soil hydrology*. Catena-Verlag, Cremlingen-Destedt, Germany. *Soil hydrology*. Catena-Verlag, Cremlingen-Destedt, Germany.
- Liao, Z., Hong, Y., Wang, J., Fukuoka, H., Sassa, K., Karnawati, D., & Fathani, F. (2010). Prototyping an experimental early warning system for rainfall-induced landslides in Indonesia using satellite remote sensing and geospatial datasets. *Landslides*, 7(3), 317–324. <https://doi.org/10.1007/s10346-010-0219-7>
- Lin, C. W., Liu, S. H., Lee, S. Y., & Liu, C. C. (2006). Impacts of the Chi-Chi earthquake on subsequent rainfall-induced landslides in central Taiwan. *Engineering Geology*, 86(2–3), 87–101. <https://doi.org/10.1016/j.enggeo.2006.02.010>
- Liu, D. L., Zhang, S. J., Yang, H. J., Zhao, L. Q., Jiang, Y. H., Tang, D., & Leng, X. P. (2016). Application and analysis of debris-flow early warning system in Wenchuan earthquake-affected area, 483–496. <https://doi.org/10.5194/nhess-16-483-2016>
- Mathew, J., Babu, D. G., Kundu, S., Kumar, K. V., & Pant, C. C. (2014). Integrating intensity-duration-based rainfall threshold and antecedent rainfall-based probability estimate towards generating early warning for rainfall-induced landslides in parts of the Garhwal Himalaya, India. *Landslides*, 11(4), 575–588. <https://doi.org/10.1007/s10346-013-0408-2>
- MoHA. (2011). *Nepal Disaster Report*. Retrieved from [http://www.moha.gov.np/uploads/document/file/Nepal\\_Disaster\\_Report\\_2011\\_2013090403124](http://www.moha.gov.np/uploads/document/file/Nepal_Disaster_Report_2011_2013090403124)

2.pdf

- Saxton, K., & Rawls, W. (2006). Soil Water Characteristic Estimates by Texture and Organic Matter for Hydrologic Solutions. *Soil Science Society of America Journal*, 70, 1569–1578. <https://doi.org/10.2136/sssaj2005.0117>
- Schaap, M. G. (1999). Rosetta Manual. US Salinity Laboratory: Riverside, CA.
- Staehli, M., Saettele, M., Huggel, C., McArdell, B. W., Lehmann, P., Van Herwijnen, A., ... Springman, S. M. (2015). Monitoring and prediction in early warning systems for rapid mass movements. *Natural Hazards and Earth System Sciences*, 15(4), 905–917. <https://doi.org/10.5194/nhess-15-905-2015>
- Survey Department Government of Nepal. (1996). *Topographic map of Rasuwa*.
- Tang, C., Zhu, J., Li, W. L., & Liang, J. T. (2009). Rainfall-triggered debris flows following the Wenchuan earthquake. *Bulletin of Engineering Geology and the Environment*, 68(2), 187–194. <https://doi.org/10.1007/s10064-009-0201-6>
- The Government of Nepal - Ministry of Home Affairs (MoHA) and Disaster Preparedness Network-Nepal (DPNet-Nepal). (2015). *Nepal disaster report 2015*. <https://doi.org/10.1017/CBO9781107415324.004>
- Thiebes, B., Bell, R., Glade, T., Jäger, S., Mayer, J., Anderson, M., & Holcombe, L. (2014). Integration of a limit-equilibrium model into a landslide early warning system. *Landslides*, 11(5), 859–875. <https://doi.org/10.1007/s10346-013-0416-2>
- Tien Bui, D., Pradhan, B., Lofman, O., Revhaug, I., & Dick, Ø. B. (2013). Regional prediction of landslide hazard using probability analysis of intense rainfall in the Hoa Binh province, Vietnam. *Natural Hazards*, 66(2), 707–730. <https://doi.org/10.1007/s11069-012-0510-0>
- van Beek, L. P. H. (2002). *Assessment of the influence of changes in land use and climate on landslide activity in a Mediterranean environment*.
- Wang, J. (2011). *Experimental Research on Shear Parameter of High Cut Slope Gravel Soil in Badong and Its Engineering Application*. China Three Gorges University.
- world weather online. (n.d.). Retrieved November 10, 2016, from <https://www.worldweatheronline.com/rasuwa-weather-averages/np.aspx>
- Xu, W.-J., Xu, Q., & Hu, R.-L. (2011). Study on the shear strength of soil-rock mixture by large scale direct shear test. *International Journal of Rock Mechanics and Mining Sciences*, 48(8), 1235–1247. <https://doi.org/10.1016/j.ijrmms.2011.09.018>
- Yang, T. (2013). *Study on effects of physical properties on mechanical behaviors of gravel soil*. Southwest Jiaotong University.
- Zhong, R., Yuhua, B., Xiubin, H., & Jinzhang, G. (2015). Root Tensile Properties and Root Cohesion of 4 herbaceous Plant Species in the Riparian Zone of Three Gorges Reservoir. *Journal of Soil and Water Conservation*, 29(4), 188–194. <https://doi.org/10.13870/j.chki.stbcxb.2015.04.035>
- Zhou, W., & Tang, C. (2014). Rainfall thresholds for debris flow initiation in the Wenchuan earthquake-stricken area, southwestern China. *Landslides*, 11(5), 877–887. <https://doi.org/10.1007/s10346-013-0421-5>



## APPENDIX

Appendix 1 soil samples information

Name	Location	Depth	Gravel	Description
Sample 1	Near Dhunche	0-20cm	1-3cm, 15%	Farming soil, brown, with vegetation roots, high organic material, vegetation covered
Sample 2	Mukharka	0-30cm (middle layer)	5-8cm, 30%(sample did not take large gravels, )	Colluvial material, brown, high gravel content, left side surface
Sample 3	Grang	0-20cm (top layer)	1-3cm, 40%	Colluvial deposit, grey, high gravel content, in slip mass
Sample 4	Ramche	0-20cm	0.5-2cm, 30%	Farm land, light brown, with roots, many small gravels, vegetation covered
Sample 5	Kalikasthan	0-10cm (top-middle layer)	0.5-5cm, 50% (sample did not take large gravels, )	Debris flow /colluvial deposit, brown to gray, many small fragmentized gravels, galley with large amounts of water.
Sample 6	Mailong	10-20cm (top layer)	1-4cm, 50% (sample did not take large gravels, )	Colluvial deposit, fresh surface may be activated in 2016, brown to gray, the stone has a very sharp edge, many big size stone nearby.
Sample 7	Kalikasthan ECO-DRR	0-20cm	0.5-1 cm	Wild soil, ECO part, with root and organic material,

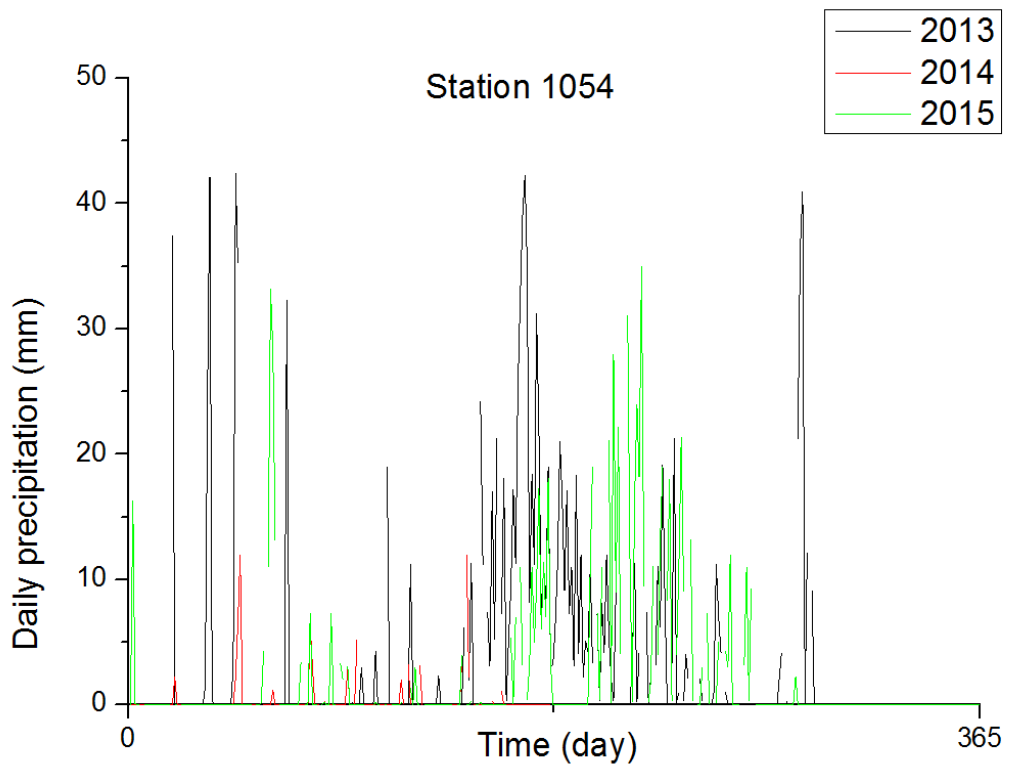
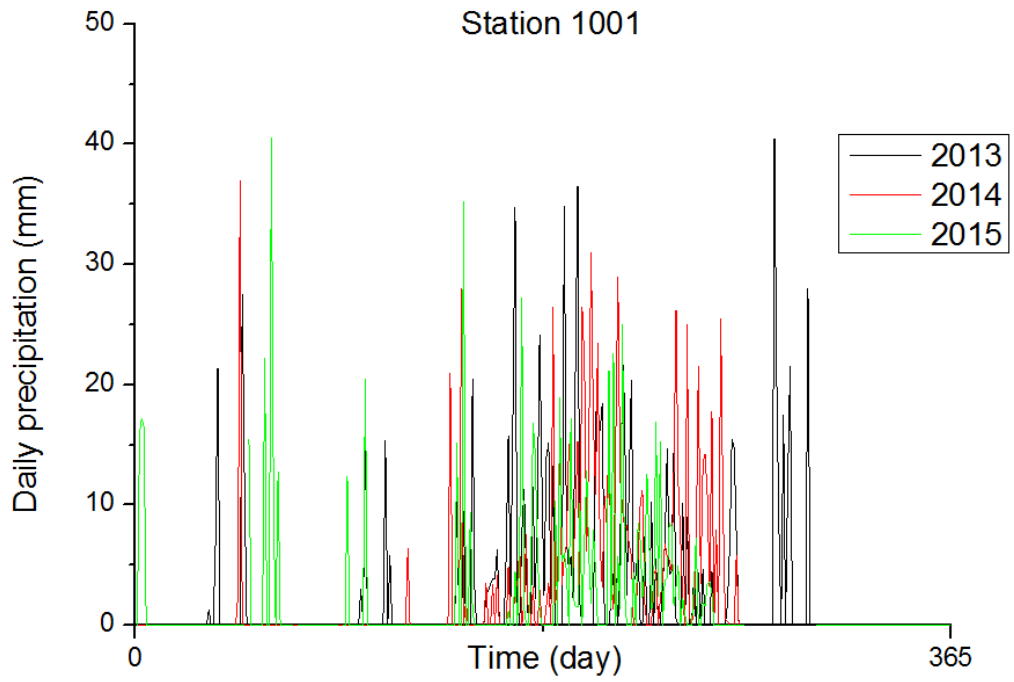
Appendix 2 Table of soil test results

No	Classification	Location	Sand content % (excluding gravels)	Organic content %	Gravel content %	compaction	Ksat mm/hour
1	farm	Near Dhunche	0.9	5	15	Loose-normal	28.8
2	deep	Mukharka	0.82	1	30	Dense	36
3	middle	Grang	0.82	1	40	Hard	7.2
4	farm	Ramche	0.89	5	30	Normal	18
5	middle-deep	Kalikasthan	0.82	1	50	Dense	14.4
6	middle	Mailong	0.85	1	50	Dense	10.8
7	farm	Kalikasthan	0.9	5	10	Loose-normal	28.8

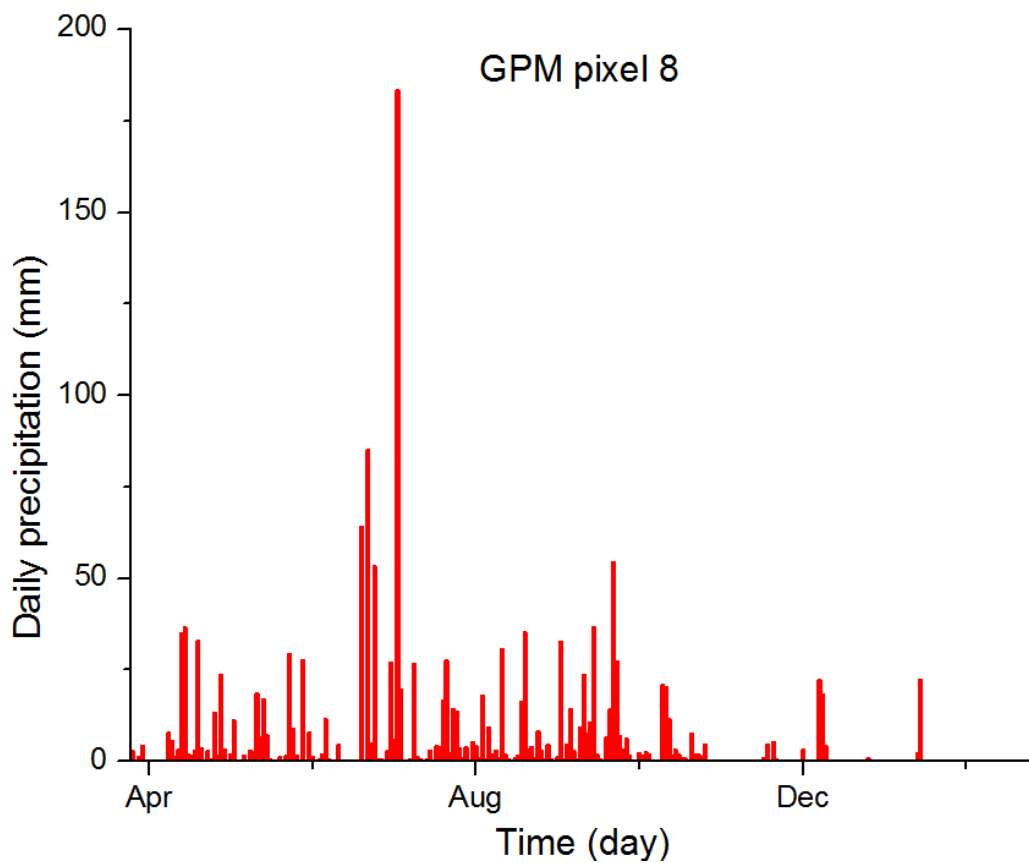
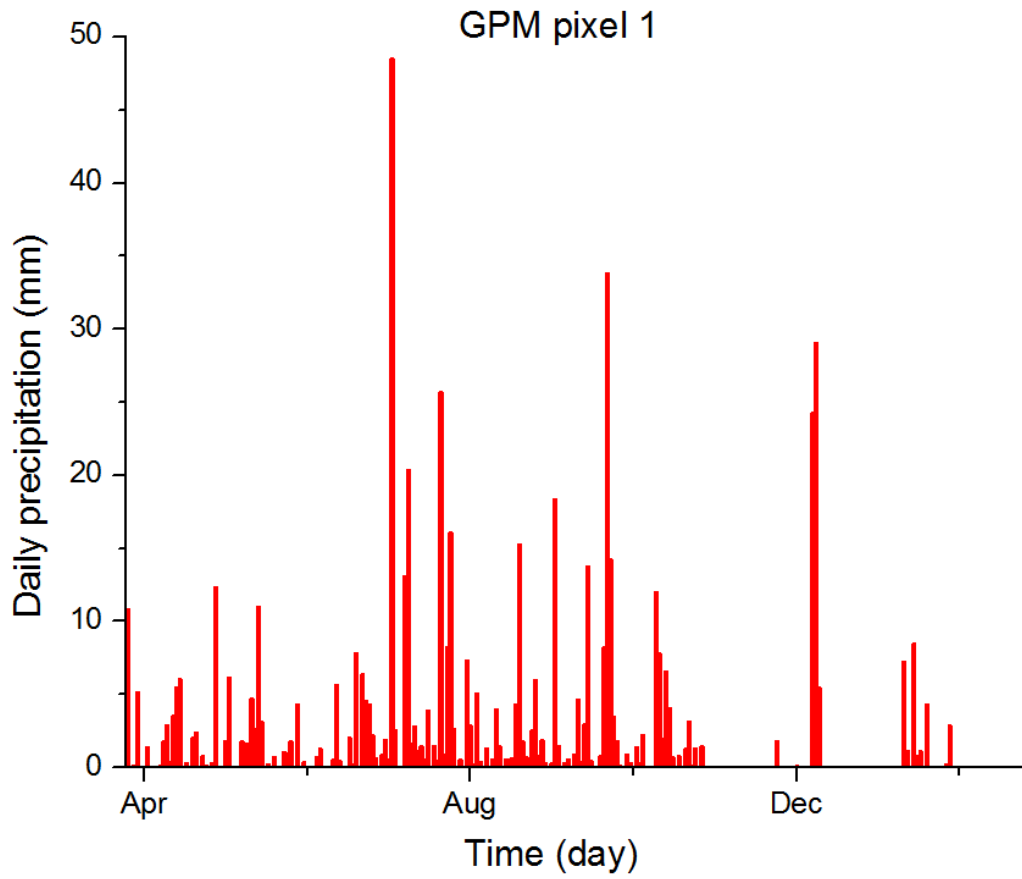
Appendix 3 Correlation analysis table.

	GPM 1	GPM 2	GPM 3	GPM 4	GPM 5	GPM 6	GPM 7	GPM 8	GPM 9	1001	1054	1057	1055	1058	1004	1017	TRMM
GPM 1	PCC	1.00	0.96	0.87	0.91	0.81	0.77	0.78	0.72	0.49	-0.01	0.09	0.30	0.32	0.18	-0.03	0.09
GPM 1	Sig.	--	0.00	0.00	0.00	0.00	0.00	0.00	0.00	0.00	0.90	0.34	0.00	0.00	0.06	0.74	0.32
GPM 2	PCC	0.96	1.00	0.92	0.90	0.85	0.76	0.79	0.71	0.44	-0.01	0.10	0.24	0.26	0.17	-0.02	0.10
GPM 2	Sig.	0.00	--	0.00	0.00	0.00	0.00	0.00	0.00	0.00	0.93	0.27	0.01	0.00	0.07	0.85	0.26
GPM 3	PCC	0.87	0.92	1.00	0.80	0.94	0.72	0.78	0.75	0.39	0.02	0.11	0.21	0.26	0.11	0.03	0.08
GPM 3	Sig.	0.00	0.00	--	0.00	0.00	0.00	0.00	0.00	0.00	0.87	0.22	0.02	0.00	0.26	0.76	0.38
GPM 4	PCC	0.91	0.90	0.80	1.00	0.85	0.92	0.92	0.80	0.47	0.00	0.03	0.27	0.27	0.17	-0.04	0.18
GPM 4	Sig.	0.00	0.00	0.00	--	0.00	0.00	0.00	0.00	0.00	0.97	0.73	0.00	0.00	0.07	0.66	0.05
GPM 5	PCC	0.90	0.94	0.86	0.97	1.00	0.90	0.92	0.80	0.43	0.00	0.05	0.22	0.22	0.18	-0.03	0.16
GPM 5	Sig.	0.00	0.00	0.00	0.00	--	0.00	0.00	0.00	0.00	1.00	0.60	0.01	0.02	0.06	0.75	0.07
GPM 6	PCC	0.81	0.85	0.94	0.85	1.00	0.84	0.89	0.87	0.35	-0.02	0.03	0.20	0.21	0.15	0.00	0.11
GPM 6	Sig.	0.00	0.00	0.00	0.00	--	0.00	0.00	0.00	0.00	0.87	0.76	0.03	0.02	0.11	0.96	0.24
GPM 7	PCC	0.77	0.76	0.72	0.92	0.84	1.00	0.98	0.90	0.40	0.00	0.02	0.25	0.24	0.18	-0.02	0.19
GPM 7	Sig.	0.00	0.00	0.00	0.00	0.00	--	0.00	0.00	0.00	0.98	0.86	0.01	0.01	0.06	0.82	0.04
GPM 8	PCC	0.78	0.79	0.78	0.92	0.89	0.98	1.00	0.91	0.41	0.02	0.02	0.24	0.24	0.18	-0.01	0.19
GPM 8	Sig.	0.00	0.00	0.00	0.00	0.00	0.00	--	0.00	0.00	0.83	0.83	0.01	0.01	0.06	0.93	0.03
GPM 9	PCC	0.72	0.71	0.75	0.80	0.87	0.90	0.91	1.00	0.38	0.00	0.04	0.30	0.27	0.21	0.03	0.14
GPM 9	Sig.	0.00	0.00	0.00	0.00	0.00	0.00	0.00	--	0.00	0.99	0.64	0.00	0.00	0.03	0.72	0.12
1001	PCC	0.49	0.44	0.39	0.47	0.35	0.40	0.41	0.38	1.00	0.28	0.11	0.45	0.50	0.17	0.13	0.04
1001	Sig.	0.00	0.00	0.00	0.00	0.00	0.00	0.00	0.00	--	0.01	0.23	0.00	0.00	0.07	0.16	0.65
1054	PCC	-0.01	-0.01	0.02	0.00	-0.02	0.00	0.02	0.00	0.28	1.00	0.14	0.14	0.05	0.14	0.24	0.09
1054	Sig.	0.90	0.93	0.87	0.97	0.87	0.98	0.83	0.99	0.01	--	0.16	0.17	0.63	0.18	0.02	0.37
1057	PCC	0.09	0.10	0.11	0.03	0.03	0.02	0.02	0.04	0.11	0.14	1.00	0.03	0.28	0.00	0.24	0.26
1057	Sig.	0.34	0.27	0.22	0.73	0.60	0.86	0.83	0.64	0.23	0.16	--	0.71	0.00	1.00	0.01	0.00
1055	PCC	0.30	0.24	0.21	0.27	0.22	0.25	0.24	0.30	0.45	0.14	0.03	1.00	0.31	0.19	0.27	0.01
1055	Sig.	0.00	0.01	0.02	0.00	0.01	0.01	0.01	0.00	0.00	0.17	0.71	--	0.00	0.05	0.00	0.92
1058	PCC	0.32	0.26	0.26	0.27	0.22	0.21	0.24	0.27	0.50	0.05	0.28	0.31	1.00	0.20	0.20	0.04
1058	Sig.	0.00	0.00	0.00	0.00	0.02	0.01	0.01	0.00	0.00	0.63	0.00	0.00	--	0.04	0.03	0.70
1004	PCC	0.18	0.17	0.11	0.17	0.15	0.18	0.18	0.21	0.17	0.14	0.00	0.19	0.20	1.00	0.44	0.11
1004	Sig.	0.06	0.07	0.26	0.07	0.11	0.06	0.06	0.03	0.07	0.18	1.00	0.05	0.04	--	0.00	0.23
1017	PCC	-0.03	-0.02	0.03	-0.04	0.00	-0.02	-0.01	0.03	0.13	0.24	0.24	0.27	0.20	0.44	1.00	0.18
1017	Sig.	0.74	0.85	0.76	0.66	0.96	0.82	0.93	0.72	0.16	0.02	0.01	0.00	0.03	0.00	--	0.05
TRMM	PCC	0.09	0.10	0.08	0.18	0.11	0.19	0.19	0.14	0.04	0.09	0.26	0.01	0.04	0.11	0.18	1.00
TRMM	Sig.	0.32	0.26	0.38	0.05	0.07	0.04	0.03	0.12	0.65	0.37	0.00	0.92	0.70	0.23	0.05	--

Appendix 4 Examples of 2015 rainfall station data



Appendix 5 Examples of 2015 GPM satellite data (from April 1<sup>st</sup>)



Appendix 6 Some input of STARWAR+PROBSTAB model

